© 2016. Published by The Company of Biologists Ltd | Development (2016) 143, 1800-1810 doi:10.1242/dev.130039

RESEARCH ARTICLE

Reiterative expression of *pax1* directs pharyngeal pouch segmentation in medaka

Kazunori Okada[1,2,*,‡], Keiji Inohaya[3], Takeshi Mise[1], Akira Kudo[3], Shinji Takada[2,4,‡] and Hiroshi Wada[1,‡]

ABSTRACT

A striking characteristic of vertebrate development is the pharyngeal arches, which are a series of bulges on the lateral surface of the head of vertebrate embryos. Although each pharyngeal arch is segmented by the reiterative formation of endodermal outpocketings called pharyngeal pouches, the molecular network underlying the reiterative pattern remains unclear. Here, we show that *pax1* plays crucial roles in pouch segmentation in medaka (*Oryzias latipes*) embryos. Importantly, *pax1* expression in the endoderm prefigures the location of the next pouch before the cells bud from the epithelium. TALEN-generated *pax1* mutants did not form pharyngeal pouches posterior to the second arch. Segmental expression of *tbx1* and *fgf3*, which play essential roles in pouch development, was almost non-existent in the pharyngeal endoderm of *pax1* mutants, with disturbance of the reiterative pattern of *pax1* expression. These results suggest that *pax1* plays a key role in generating the primary pattern for segmentation in the pharyngeal endoderm by regulating *tbx1* and *fgf3* expression. Our findings illustrate the crucial roles of *pax1* in vertebrate pharyngeal segmentation and provide insights into the evolutionary origin of the deuterostome gill slit.

KEY WORDS: Pharyngeal arch, Pharyngeal pouch, Gill slit, Segmentation, Evolution, *Pax1*

INTRODUCTION

The metamerism of vertebrate pharyngeal structures, such as the skeletal elements of jaws, gills and cranial nerve projections, originates from segmental development of the pharyngeal arches, which are transient embryonic structures seen in all vertebrate embryos (Graham and Richardson, 2012). The pharyngeal arches are formed from all three germ layers, and the cranial neural crest cells were traditionally thought to play a crucial role in arch segmental development (Noden, 1988). However, experimental ablation of the cranial crest cells does not affect segmental development of the reiterative endodermal outpocketings (called pharyngeal pouches) or the expression patterns of *Bmp7*, *Fgf8*, *Shh* and *Pax1* in the pouches (Veitch et al., 1999).

[1]Graduate School of Life and Environmental Sciences, University of Tsukuba, 111 Tennoudai, Tsukuba 305-8572, Japan. [2]Okazaki Institute for Integrative Bioscience and National Institute for Basic Biology, National Institutes of Natural Sciences, 5-1 Higashiyama, Myodaiji-cho, Okazaki 444-8787, Japan. [3]Department of Biological Information, Tokyo Institute of Technology, 4259 Nagatsuta, Midori-ku, Yokohama 226-8501, Japan. [4]Department for Basic Biology, SOKENDAI (The Graduate University for Advanced Studies), 5-1 Higashiyama, Myodaiji-cho, Okazaki 444-8787, Japan.
*Present address: Okazaki Institute for Integrative Bioscience and National Institute for Basic Biology, National Institutes of Natural Sciences, 5-1 Higashiyama, Myodaiji-cho, Okazaki 444-8787, Japan.

‡Authors for correspondence (tobiuo126@gmail.com; stakada@nibb.ac.jp; hwada@biol.tsukuba.ac.jp)

Received 19 August 2015; Accepted 21 March 2016

Numerous studies have reported the roles of different signaling molecules and transcription factors in pouch segmentation. Retinoic acid (RA), a morphogen that globally regulates vertebrate head development, is required for posterior pouch segmentation in mice (Wendling et al., 2000), quail (Quinlan et al., 2002), zebrafish (Kopinke et al., 2006) and lamprey (Kuratani et al., 1998) (a jawless vertebrate). FGF signaling also contributes to pouch segmentation in both gnathostomes (jawed vertebrates) and lamprey (Abu-Issa et al., 2002; Crump et al., 2004; Jandzik et al., 2014). In zebrafish, pouch-specific expression of *fgf3* is considered to be responsible for endodermal pouch patterning as well as subsequent chondrogenesis (David et al., 2002; Crump et al., 2004; Herzog et al., 2004). The indispensable role of *Tbx1* in pharyngeal segmentation was revealed through studies using mouse and zebrafish mutants that sought to identify candidate genes involved in DiGeorge syndrome (Jerome and Papaioannou, 2001; Piotrowski et al., 2003; Xu et al., 2005). *Tbx1* is expressed in the pharyngeal ectoderm, endoderm and mesoderm (Chapman et al., 1996; Vitelli et al., 2002; Piotrowski et al., 2003). In mice, although mesodermal *Tbx1* is required for proper pouch development (Zhang et al., 2006), dynamic expression of *Ripply3*, which encodes a Tbx1 repressor, regulates the endodermal activity of Tbx1 to form pouches posterior to the second arch (Okubo et al., 2011). In zebrafish, mesodermal *tbx1* drives endodermal pouch morphogenesis by upregulating the expression of *wnt11r* and *fgf8* in a cell-autonomous manner (Choe and Crump, 2014). It was also reported that the segmental expression pattern of *fgf3* is retained in the pharyngeal endoderm of *tbx1* mutants and that both mesodermal and endodermal Tbx1 play roles ensuring proper pouch segmentation (Choe and Crump, 2014). Therefore, the regulatory network for the endodermal expression of *tbx1* and *fgf3* is crucial for generating the reiterative pattern of pharyngeal segmentation. However, we know little about the molecular mechanisms of segmental pattern formation in the pharyngeal endoderm, especially regarding regulation of the endodermal expression of *tbx1* and *fgf3*.

Endodermal pharyngeal pouches are not specific to vertebrates but are common in deuterostome animals, including fossil echinoderms (Clausen and Smith, 2005), as pharyngeal gill slits. Previous studies demonstrated the remarkable conservation of the expression patterns of genes governing the development of vertebrate pharyngeal pouches and the gill slits of non-vertebrate deuterostomes, clearly illustrating the homology between these structures (Holland et al., 1995; Müller et al., 1996; Wallin et al., 1996; Ogasawara et al., 1999, 2000; Lowe et al., 2003; Gillis et al., 2012). Therefore, revealing the mechanism of segmented pharyngeal pouch formation is indispensable for shedding light on not only vertebrate developmental principles but also the evolutionary origins of the vertebrate body plan (Graham et al., 2014).

In this study, we focused on *pax1*, which encodes a paired-box transcription factor. Conserved expression of *pax1/9* homologs in

Development (2016) 143, 1800-1810 doi:10.1242/dev.130039

pharyngeal gill slits provides key evidence of the homology between deuterostome gill slits and pharyngeal pouches (Holland et al., 1995; Müller et al., 1996; Wallin et al., 1996; Ogasawara et al., 1999, 2000; Lowe et al., 2003; Gillis et al., 2012). Previous reports clearly demonstrated the developmental functions of *Pax1* in organogenesis of the thymus and parathyroid glands, sclerotome delineation, chondrogenesis and vertebral column formation (Wallin et al., 1996; Peters et al., 1999; Su et al., 2001; Mise et al., 2008). These studies were undertaken in mice, but no studies have elucidated the function of *Pax1* in pharyngeal pouch segmentation, as the reiterative pouches are retained even in the endoderm of *Pax1;Pax9* double-knockout mice (Zou et al., 2006). Previously, we unexpectedly identified a crucial function of *pax1* in pouch segmentation in medaka (Mise et al., 2008). Here, we show that the expression pattern of *pax1* is dynamic and prefigures the future location of pouches. We analyzed *pax1* mutant medaka generated by TALEN-mediated mutagenesis and reveal the indispensable functions of *pax1* in both the reiterative expression of *tbx1* and *fgf3* in the pharyngeal endoderm forming posterior to the second arch and in subsequent pouch segmentation.

RESULTS

Roles of *pax1* in formation of the segmental structures of the medaka pharynx

Teleost embryos develop seven pharyngeal arches. Starting from the anterior end, the first (or mandibular) arch develops Meckel's and palatoquadrate mandibular cartilages (Fig. 1A). The second (or hyoid) arch contributes to the basihyal, ceratohyal and hyosymplectic cartilages, and the third to seventh arches give rise to a series of ceratobranchial and basibranchial cartilages (Fig. 1A). All *pax1* mutant larvae exhibited complete loss of the ceratobranchial cartilages, except for the most posterior (seventh) arch with pharyngeal teeth. The basibranchial cartilage of pharyngeal arches 3-6 was highly deformed (Fig. 1B, Table S2). Although other pharyngeal cartilages were retained, a hole in the dorsal plate of the hyosymplectic cartilage was often lost in *pax1* mutants (Fig. 1B, Table S2). In addition to such deformation, the hyosymplectic and ceratohyal cartilages were sometimes fused (Fig. 1B, Table S2). By contrast, the components of the mandibular arch rarely exhibited abnormalities (Fig. 1B, Table S2).

The cranial nerve is another structure that exhibits segmental organization, projecting itself into each pharyngeal arch (Fig. 1C). Of the ten cranial nerves in teleosts, cranial nerves V (trigeminal), VII (facial), XI (glossopharyngeal) and X (vagus) run into distinct pharyngeal arches (Fig. 1C). In *pax1* mutants, projections of cranial nerves IX and X were specifically suppressed, whereas projections of cranial nerves V and VII were unaffected (Fig. 1D). The innervation of cranial nerve IX was less affected than the branches of cranial nerve X, but its destination was the dorsal area of the second arch rather than its normal projection into the third arch (Fig. 1D, arrowhead and lower panel).

Additionally, we examined the expression of *foxN1*, which is normally detected in the thymus primordium (Li et al., 2007) (Fig. 1E). In *pax1* mutants, thymus-specific expression of *foxN1* was lost (Fig. 1F). As these mutant phenotypes are often associated with pharyngeal pouch defects, we further investigated the expression pattern and function of *pax1* during pharyngeal pouch segmentation.

Expression of *pax1* prefigures the location of future pouches

In order to document the role of *pax1* in the pharyngeal endoderm, we examined a detailed temporal profile of *pax1* expression. At early stage 21 (corresponding to the 8-somite stage), *pax1* expression was observed in the lateral cells of the anterior pharyngeal endoderm (Fig. 2A). More posteriorly, expression was also observed in bilateral spots of cells (Fig. 2A). Compared with the endodermal expression of *foxA2*, these posterior spots seemed to mark locations for cells to bud off to form the following pouch (Fig. 2A-E). We also detected endoderm-specific pharyngeal expression of *pax1* by double-fluorescence *in situ* hybridization for *pax1* and other marker genes (Fig. 3). At late stage 22 (the 10-somite stage), *pax1* expression specifically marked the first and second pouches (Fig. 2F,G). Notably, other bilateral spots of *pax1* expression were detected in a posterior region relative to the second pouch (Fig. 2F,H,I, arrowheads). As the pharyngeal pouches

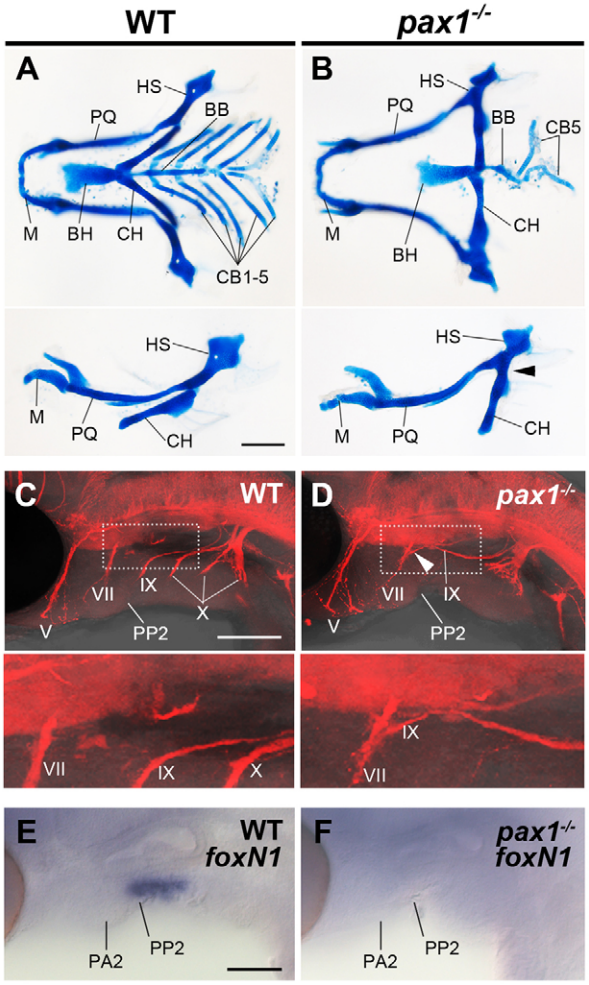

Fig. 1. Roles of *pax1* in the gill cartilages, cranial nerve projections and thymus primordium. (A,B) Flat-mount views of pharyngeal cartilages (top row) and left-side views of mandibular and hyoid elements (bottom row) in wild-type and *pax1* mutant medaka larvae 2 days after hatching. The joint between HS and CH cartilages is often fused in the mutant larvae (B, arrowhead). (C,D) Whole-mount immunohistochemistry of medaka embryos at 3 days postfertilization with anti-acetylated tubulin antibody. In *pax1* mutants, projections of cranial nerves V and VII are present, but IX fails to project to the correct position (D, arrowhead), and branches of cranial nerve X do not exhibit the segmental trajectories (n=13). The boxed regions are shown at higher magnification beneath. (E,F) Expression of *foxN1* in the pharynx of wild type and *pax1* mutant. (E) In the wild type, *foxN1* expression was present in cells of the thymus primordium. (F) However, no pharyngeal expression of *foxN1* was detected in the *pax1* mutant (n=15). BB, basibranchial; BH, basihyal; CB, ceratobranchial; CH, ceratohyal; HS, hyosymplectic; M, Meckel's; PQ, palatoquadrate; PP2, the second pharyngeal pouch; PA2, the second pharyngeal arch. Scale bars: 100 µm in A-D; 50 µm in E,F.

Development (2016) 143, 1800-1810 doi:10.1242/dev.130039

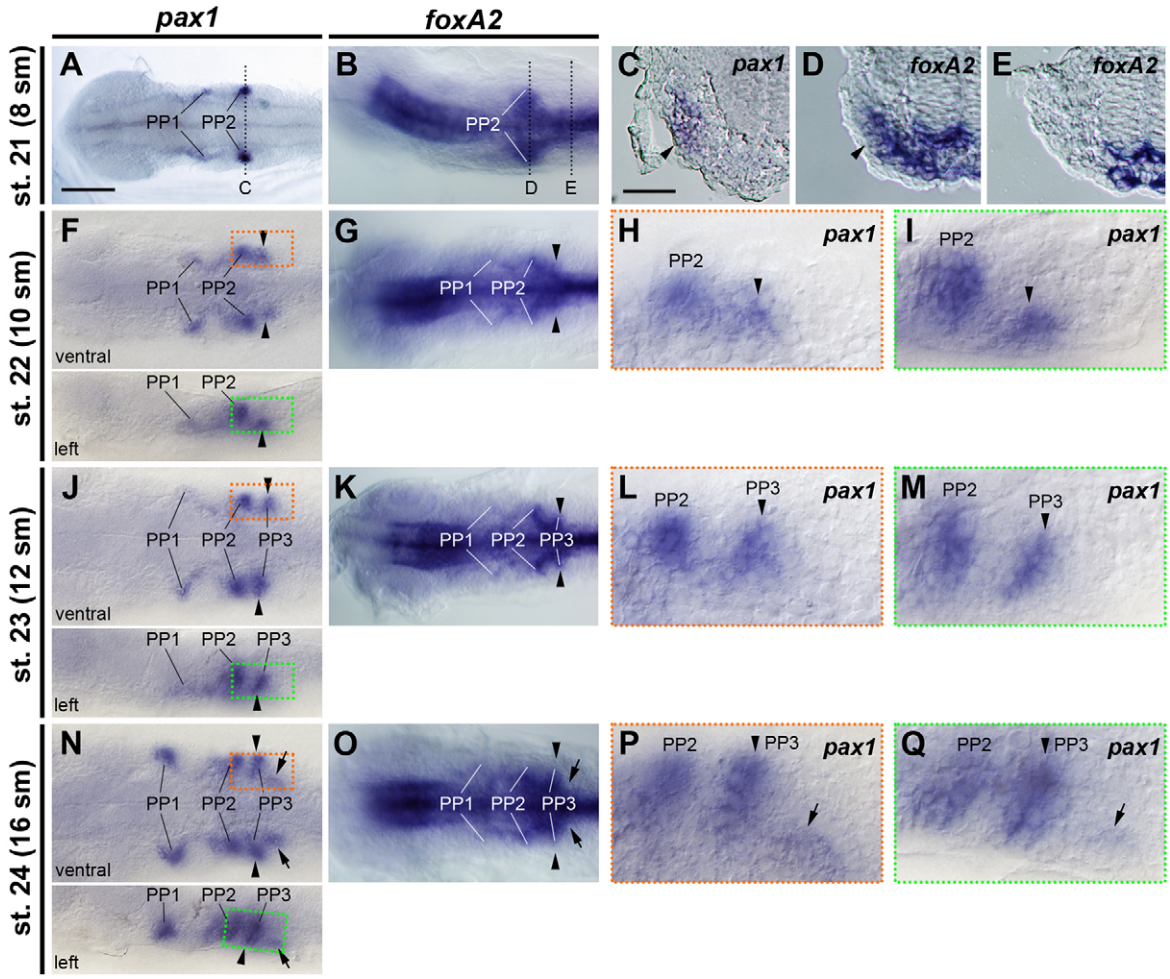

Fig. 2. Reiterative expression of *pax1* and pharyngeal pouch segmentation. (A,C,F,H-J,L-N,P,Q) Expression of *pax1* during pouch development marks the pharyngeal pouches and prefigures the endodermal positions where the next pouches will be formed. (B,D,E,G,K,O) *foxA2* is expressed in the pharyngeal endoderm and marks the pharyngeal pouches. Whole-mount embryos observed from the ventral (A,B,G,H,K,L,O,P and upper panels of F,J,N) and left side (I,M,Q and lower panels of F,J,N). High-magnification images of the orange (H,L,P) and green (I,M,Q) boxed regions in F,J,N, respectively, are shown. Arrowheads (F-Q) indicate PP3 or presumptive PP3. Arrows (N-Q) indicate presumptive PP4. (C-E) Transverse sections at the axial levels shown in A and B (dotted lines). These sections show that *pax1* is expressed in the pouch endoderm (arrowhead in C) and that *foxA2* is expressed in the pouch (arrowhead in D) and non-pouch endoderm (E). PP, pharyngeal pouch; sm, somite. Scale bars: 100 µm, except 50 µm in C-E.

develop in an oblique manner along the dorsoventral axis, the signal appeared continuous from the second pouch in the ventral view (Fig. 2F,H). A lateral view clearly indicated that the posterior *pax1*-positive cells were separated from the *pax1*-positive anterior pouch cells (Fig. 2F,I, arrowheads). This posterior expression might mark cells of the nascent third pouch, as at stage 23 (the 12-somite stage) the most posterior expression of *pax1* was detected in the third pouch (Fig. 2J-M, arrowheads). At stage 24 (the 16-somite stage), the bilateral spots of *pax1* expression appeared just posterior to the third pouch (Fig. 2N-Q, arrows). This expression is presumed to mark the next (fourth) pouch region (Fig. 2N,P,Q, arrows). Continuous *pax1*-positive domains ranging over the emerging pouch were not observed at any stage. These results suggest that *pax1* expression prefigures the position where the next pouch will be formed during the serial reiteration of posterior pouch development.

Reiterative development of the third and posterior pouches requires *pax1*

In order to determine the function of *pax1* in pouch segmentation, we examined the morphology of pharyngeal pouches and arches in wild-type and $pax1^{-/-}$ medaka by analyzing marker gene expression patterns. First, we examined the endoderm by monitoring *foxA2*. In wild-type embryos at stage 23, bilayered outpocketings of endoderm epithelium were observed at the first, second and third pouches (Fig. 4A). However, in *pax1* mutants, the posterior epithelium of the second pouch failed to fold, and no outpocketing was observed posterior to it (Fig. 4B). Consistently, the expression pattern of *dlx2*, which marks neural crest cells, showed that neural crest cells failed to segregate into segments posterior to the third arch in *pax1* mutants, perhaps owing to the third pouch defect (Fig. 4C,D). The defects in pouch segmentation were more evident at stage 27 (the stage of fifth pouch formation), when *pax1* mutant embryos never exhibited segmental pouches at the axial level of the third or posterior pouches (Fig. 4E,F). A few irregular slits forming posterior to the second arch were found in *pax1* mutants at stage 27 (Fig. S2A-F). Additionally, these mutants exhibited the normal anterior epithelial sheet of the second pouch, lining the second arch backward. However, these did not develop the bilayered morphology of the second pouch but rather a monolayer sheet (Fig. 4B,F,J, Fig. S2H). These abnormalities of the second pouch might be caused by the failure of the posterior half of the second pouch to develop. In concordance with the absence of

Development (2016) 143, 1800-1810 doi:10.1242/dev.130039

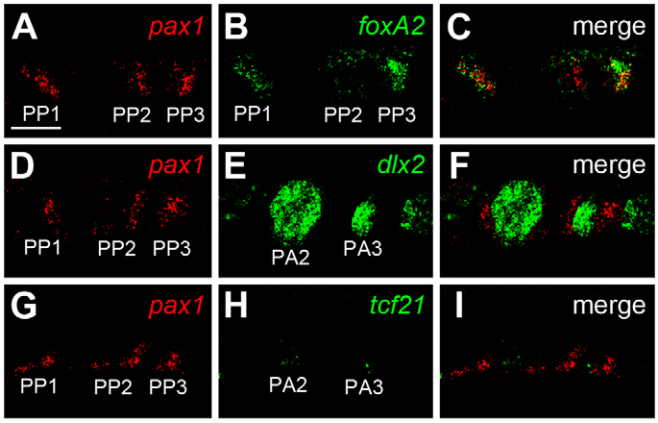

Fig. 3. Double-fluorescence *in situ* hybridization for *pax1* and marker genes. Double-fluorescence *in situ* hybridization for *pax1* and *foxA2* (A-C), *dlx2* (D-F) and *tcf21* (G-I) at stage 23. Images show the left side of embryos. Expression of *pax1* overlapped with the endodermal *foxA2* expression domain (C) but not with neural crest *dlx2* (F) or mesodermal *tcf21* (I). PA, pharyngeal arch; PP, pharyngeal pouch. Scale bar: 50 µm.

the third to fifth pouches, the segmental distribution of neural crest cells in the pharyngeal arches was disrupted in the *pax1* mutants (Fig. 4G,H). In *pax1* mutants, the crest cells were distributed so as to surround the unsegmented endodermal cells (Fig. 4G,H).

We also examined the expression patterns of other marker genes at stage 27. The expression of *nkx2.3*, which is often used as a pharyngeal pouch marker in zebrafish studies (Lee et al., 1996), showed five pairs of segmental pouches in wild-type medaka (Fig. 4I). Similar to *foxA2*, the expression of *nkx2.3* in *pax1* mutants did not show any reiterative pouch pattern, except for the first two pouches (Fig. 4J). As a mesodermal marker, we monitored the expression of *tcf21*, which is also known as *capsulin* in zebrafish (Lee et al., 2011). In *pax1* mutants, the expression of *tcf21* marked the mesodermal cores of the first and second arches, but the posterior expression never exhibited the reiterative distribution of the arch cores (Fig. 4K,L). The mesodermal distribution pattern was similar to that of the neural crest cells, despite being sparser (Fig. 4L,H). Because of the endoderm-specific expression of *pax1* in the pharynx (Fig. 3), the abnormal distribution patterns of neural crest cells and mesoderm were likely to be secondary effects of the endodermal pouch defects. These defects in pharyngeal segmentation were in complete agreement with the results of genotyping analyses of our *pax1* mutant allele (n=89/89, Fig. S1C). Additionally, a *pax1*-specific morpholino (Mise et al., 2008) phenocopied the *pax1* mutant phenotype (Fig. S3). These results rule out the possibility that off-target effects associated with TALEN caused the pharyngeal pouch defects. We therefore conclude that *pax1* plays crucial roles in the reiterative development of pharyngeal pouches forming posterior to the second arch and in the segmentation of subsequent pharyngeal pouches.

Loss of *fgf3* and *tbx1* expression in the pharyngeal endoderm of *pax1* mutants

In order to elucidate the function of *pax1* in pouch segmentation, the regulatory relationships with other segmentation genes known for their function in pharyngeal development were investigated. We first examined the effect of *pax1* on *tbx1*, which is expressed in the endoderm, mesoderm and perhaps the ectoderm of the pharynx (Piotrowski et al., 2003). At stage 24, when *pax1* expression was detected in the nascent fourth pouch endoderm (Fig. 2N-Q), *tbx1* was also expressed in the pharyngeal pouches and the posterior endoderm (Fig. 5A,C, arrowhead). In *pax1* mutants, the expression of *tbx1* in the third pouch and the fourth pouch region was dramatically reduced, although expression in the anterior pouches was unaffected (Fig. 5F). Comparison of the expression patterns of *tbx1* and endodermal *foxA2* (Fig. 5E,J) and mesodermal *tcf21* (Fig. 5B,D,G,I) revealed a clear endoderm-specific reduction in *tbx1* expression (Fig. 5F,H). At stage 27, endodermal expression of *tbx1* was detected in five pairs of pharyngeal pouches in wild-type embryos (Fig. 5K,L,O). However, except for the first and anterior half of the second pouch, almost no endodermal expression of *tbx1* was observed in *pax1* mutants (Fig. 5R,S,V). Notably, mesodermal expression of *tbx1* and *tcf21* in the *pax1* mutants was stable, indicating that the decline in *tbx1* expression in the mutant embryos was endoderm specific (Fig. 5S,T,V,W). These results suggest that the segmental expression of *tbx1* in pharyngeal pouches requires Pax1.

We also examined the expression of *fgf3*, as the skeletal pattern of *pax1* mutant medaka was almost identical to that of *fgf3*-deficient zebrafish (David et al., 2002; Herzog et al., 2004). In zebrafish, the expression of *fgf3* in the pharyngeal endoderm of *tbx1* mutants is not affected, although they lack pouch segmentation (Choe and Crump, 2014). At stage 23 in the wild type, expression of *fgf3* was detected in endodermal cells of the first, second and third pouches as well as in the midbrain-hindbrain boundary, and *fgf3* expression in the first and third pouches was much weaker than in the second pouch (Fig. 6A). In *pax1* mutants, almost no *fgf3* expression was observed in the pharyngeal pouches, including the anterior pouches (Fig. 6B, asterisks and brackets). This pouch-specific disruption in *fgf3* expression was also observed in *pax1* mutants at stage 27 (Fig. 6D, asterisks and brackets), suggesting that *pax1* is necessary for activation of the segmental expression of *fgf3* in the pharyngeal pouches. These results are consistent with our observation of skeletal defects in *pax1* mutant larvae and with the skeletal phenotypes associated with the zebrafish *fgf3* morphant and mutant (David et al., 2002; Herzog et al., 2004). Importantly, our data suggest that reiterative expression of *pax1* is crucial for the segmental expression of both *tbx1* and *fgf3* in the endoderm.

In zebrafish, *wnt11r* is reported to be expressed in the pharyngeal mesoderm in a segmental manner, and its signaling initiates the epithelial destabilization of the endoderm to form pouches (Choe et al., 2013; Choe and Crump, 2014). We therefore examined whether *wnt11r* regulates the reiterative expression of *pax1* in medaka endoderm. However, except in the mandibular arch mesoderm, no expression of *wnt11r* was detected in the pharyngeal arches of either wild-type or *pax1* mutant medaka (Fig. S4).

Loss of the reiterative pattern of *pax1* expression in the *pax1* mutant

The mutant phenotypes described above indicate that *pax1* plays a key role in establishing the primary reiterative pattern in the pharyngeal endoderm. We therefore examined the self-regulation of *pax1* expression during pharyngeal pouch segmentation. Although the expression of *pax1* in wild-type and *pax1* mutant embryos was equivalent at stage 23, remarkably, the reiterative pattern of expression changed to a continuous pattern in the *pax1* mutant while retaining independent expression in the first pouch (Fig. 7A,B). In *pax1* mutants, the expression of *pax1* in the lateral endoderm remained continuous posterior to the second arch at stage 27 (Fig. 7C,D). Examination of a horizontal section of the *pax1* mutant embryo clearly showed the continuous expression of *pax1* in the lateral endoderm where the posterior pouches failed to form (Fig. 7F).

Development (2016) 143, 1800-1810 doi:10.1242/dev.130039

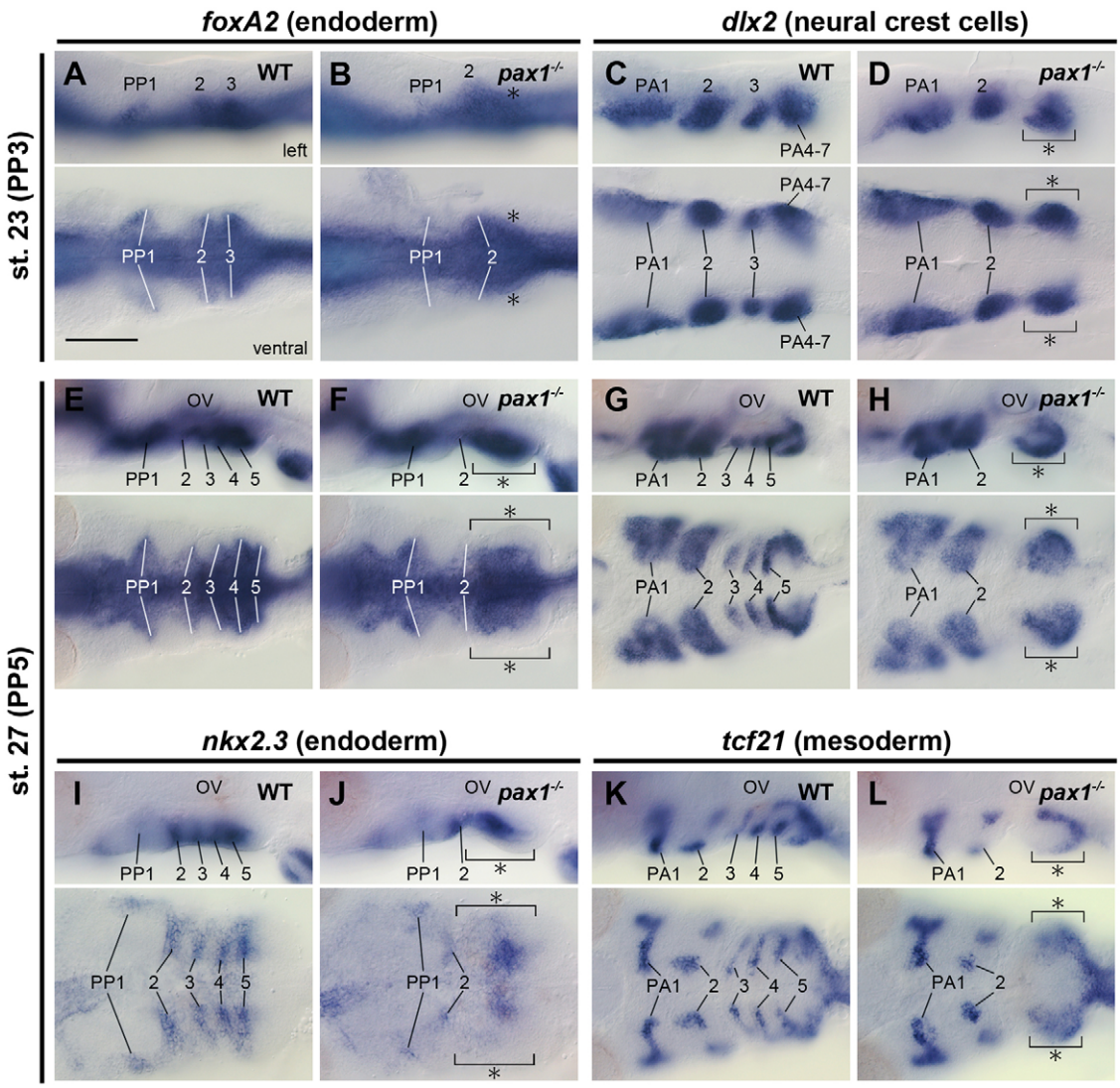

Fig. 4. Roles of *pax1* in development of the third and posterior pouches of the pharyngeal arch. (A-D) Expression of *foxA2* and *dlx2* in wild-type and *pax1* mutant embryos at stage 23. (E-L) Expression patterns of *foxA2*, *dlx2*, *nkx2.3* and *tcf21* in wild-type and *pax1* mutant embryos at stage 27. Upper and lower panels show the left side and ventral views, respectively. (A,B,E,F,I,J) The pharyngeal endoderm of the *pax1* mutant failed to form pharyngeal pouches, except for PP1 and the anterior half of PP2, as shown by the *foxA2* and *nkx2.3* expression patterns (B, *n*=4; F, *n*=18; J, *n*=4). (C,D,G,H,K,L) Expression patterns of *dlx2* and *tcf21* showed that neural crest cells (C,D,G,H) and mesodermal cells (K,L) are not divided into PA3-6 owing to the absence of PP3-5 (D, *n*=10; H, *n*=11; L, *n*=20). Asterisks and brackets indicate regions of pouch (B,F,J) or arch (D,H,L) defects associated with *pax1* deficiency. OV, otic vesicle; PA, pharyngeal arch; PP, pharyngeal pouch. Scale bar: 100 µm.

We quantified apoptotic cells in *pax1* mutants to determine whether the continuous expression of *pax1* was due to cell death in the endoderm. At stage 26, TUNEL-positive cells were found in the pharyngeal regions of both wild-type and *pax1* mutant embryos; however, no significant increase in the number of TUNEL-positive cells in the pharyngeal region was detected in the *pax1* mutants (Fig. 7G-I). Notably, continuous *pax1* expression extended to the posterior pharynx in the *pax1* mutants, where the fifth pouch forms in wild-type embryos (Fig. 7C,D). The distance from the second to the posterior end of the fifth pouch did not differ significantly between wild-type and *pax1* mutant embryos (Fig. 7J). These results indicate that *pax1* regulates its own reiterative expression pattern and that signals for the activation of *pax1* transcription might be constitutively active, with a progression to the posterior pharynx.

We also examined the expression pattern of *pax9*, a *pax1* paralog. Expression of *pax9* was detected throughout the whole area of the pharyngeal endoderm posterior to the second arch in both wild-type and in *pax1* mutant embryos (Fig. S5). Therefore, of two *pax1/9* cognates in medaka, the segmental expression pattern is specific to *pax1*.

DISCUSSION

Impact of *pax1* on pharyngeal segmentation and derivatives

Our analysis of *pax1* mutant medaka revealed the significant roles of *pax1* in the development of the pharyngeal derivatives and pouches. The severe defects in the gill cartilages and the cranial nerve branches are thought to result from the loss of *fgf3* in the pharyngeal endoderm. In zebrafish, both the *fgf3* morphant and mutant cause defects in the ceratobranchial cartilages, as seen in the *pax1* mutant medaka (David et al., 2002; Herzog et al., 2004). In zebrafish, *fgf3* is also thought to be required for cranial nerve development, as *fgf3* knockdown causes the loss of epibranchial placodes (Nechiporuk et al., 2005). Therefore, defects in the cartilages and cranial nerves in *pax1* mutant medaka are generally thought to be due to the loss of

Development (2016) 143, 1800-1810 doi:10.1242/dev.130039

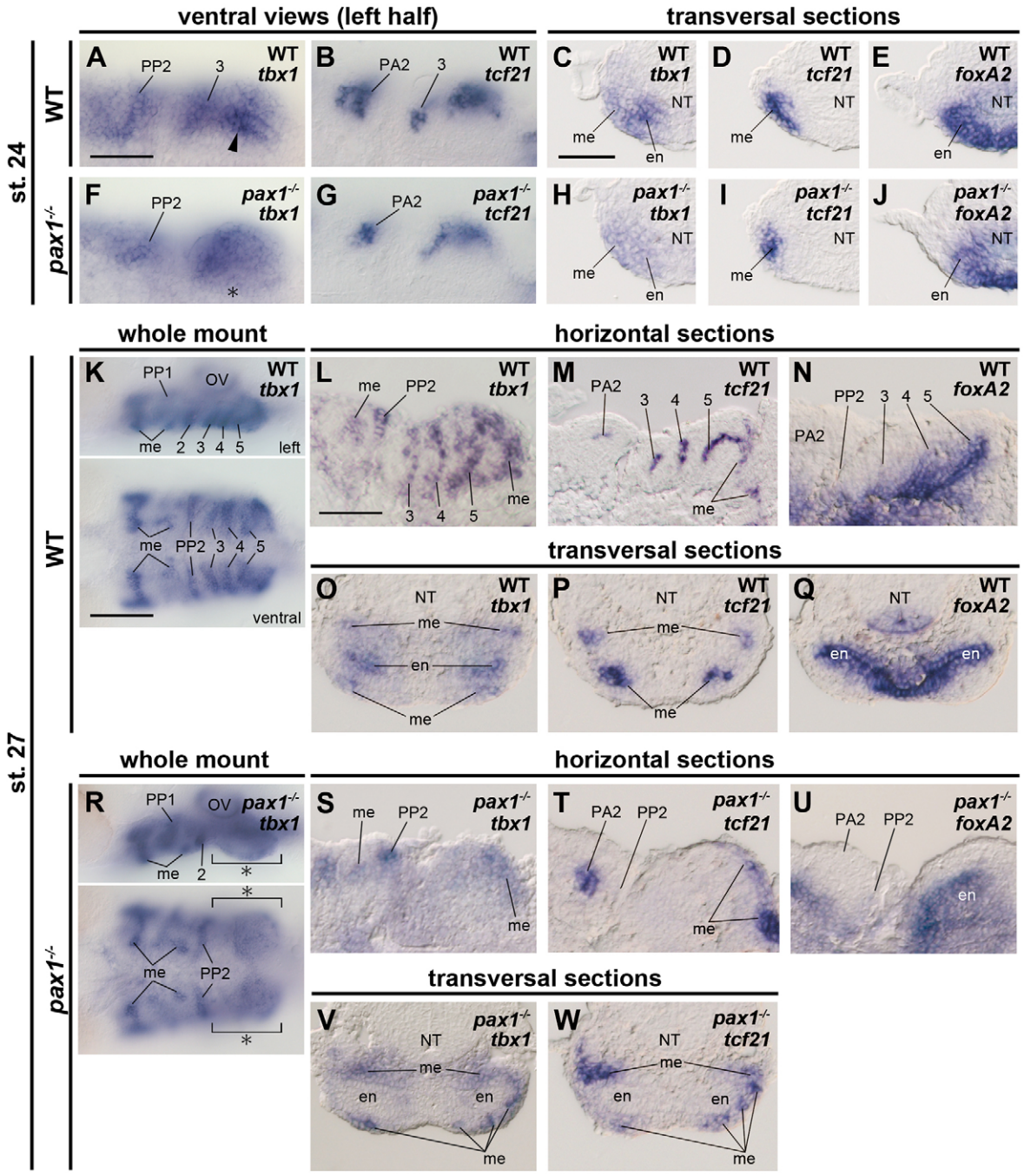

Fig. 5. Pax1 is required for endodermal expression of *tbx1*. (A-J) Expression of *tbx1* (A,C,F,H), *tcf21* (B,D,G,I) and *foxA2* (E,J) in the pharyngeal regions of wild-type (A-E) and *pax1* mutant (F-J) embryos at stage 24. (C-E,H-J) Transverse sections around the axial level of the developing fourth pouch (arrowhead in A). Endodermal expression of *tbx1* was specifically reduced in *pax1* mutant embryos, whereas mesodermal expression was retained (F,H, *n*=7). (K-W) Expression of *tbx1* (K,L,O,R,S,V), *tcf21* (M,P,T,W) and *foxA2* (N,Q,U) in the pharyngeal regions of wild-type (K-Q) and *pax1* mutant (R-W) embryos at stage 27. (K,R) Upper and lower panels show left side and ventral views, respectively. (L-N,S-U) Horizontal sections of the pharyngeal region. (O-Q,V,W) Transverse sections around the axial level of the pharynx posterior to the otic vesicle. In *pax1* mutants, endodermal expression of *tbx1* was specifically reduced posterior to PP2, whereas mesodermal expression was retained (R,S,V, *n*=18). Asterisks and brackets indicate regions affected by the loss of *pax1*. OV, otic vesicle; PA, pharyngeal arch; PP, pharyngeal pouch; me, mesoderm; en, endoderm; NT, neural tube. Scale bars: 50 µm, except 100 µm in K,R.

endodermal *fgf3*. In addition to the function of *pax1* in the pouch-specific activation of *fgf3*, our results revealed another role of *pax1* in the activation of endodermal *tbx1* segmental expression. Furthermore, *pax1* mutant medaka failed to develop the segmental pouches posterior to the second arch. Although considerable evidence demonstrates the requirement for *tbx1* and *fgf3* in pouch segmentation, the regulatory network of these genes is poorly understood. We propose a model in which the reiterative expression of *pax1* initiates segmental pouch formation by regulating *tbx1* and *fgf3* expression in the pharyngeal endoderm (Fig. 8). Importantly, *pax1* is reiteratively expressed in the nascent pouch endoderm, and the segmental expression pattern of *pax1* depends on the activity of Pax1 protein. Therefore, the reiterative pattern of *pax1* expression is probably the primary pattern for pharyngeal segmentation.

Development (2016) 143, 1800-1810 doi:10.1242/dev.130039

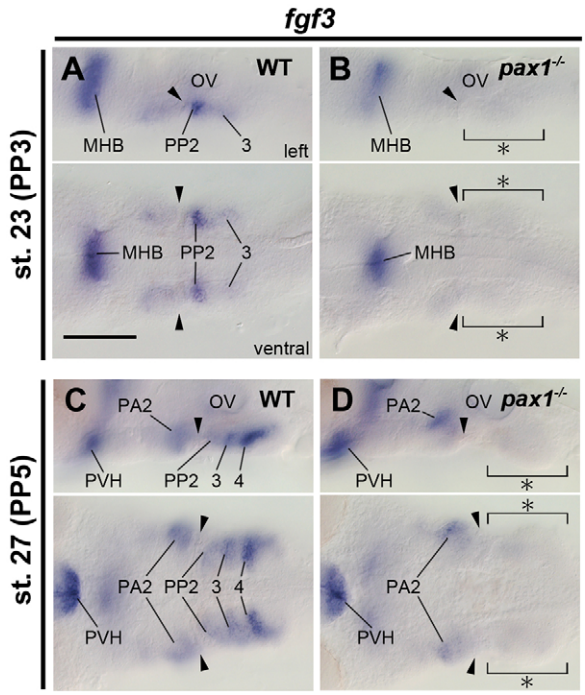

Fig. 6. Pax1 is required for endodermal expression of *fgf3*.
(A,B) Expression of *fgf3* in wild-type and *pax1* mutant embryos at stage 23. (A) Expression of *fgf3* was detected in the PP1-3 endoderm and the MHB. (B) In *pax1* mutants, expression of *fgf3* in PP1-3 was barely detected, even though expression in the MHB was retained (n=5). (C,D) Expression of *fgf3* in wild-type and *pax1* mutant embryos at stage 27. (C) In wild-type embryos, *fgf3* was expressed in the PVH, PA2 mesenchyme and PP2-4. (D) Similar to the situation at stage 23, expression of *fgf3* in the pharyngeal pouches was almost non-existent in the *pax1* mutant (n=13). Top and bottom rows show left side and ventral views, respectively. Arrowheads indicate the anterior walls of PP2. Asterisks and brackets mark regions of reduced *fgf3* expression. PA, pharyngeal arch; PP, pharyngeal pouch; MHB, midbrain-hindbrain boundary; OV, otic vesicle; PVH, posterior-ventral hypothalamus. Scale bar: 100 µm.

In the pharyngeal endoderm of the *pax1* mutant, we also observed loss of expression of *foxN1*, a gene normally expressed in cells of the thymus primordium (Li et al., 2007), indicating that *pax1* is indispensable for thymus development in medaka. Although mouse *Pax1* is necessary for proper development of the thymus epithelium, it is not sufficient for thymus development, as *Foxn1* expression was observed in *Pax1* single-mutant mice (Su et al., 2001). Even though indirect effects of the *pax1* mutation on pouch defects must be considered, our results nevertheless shed light on the significant roles of *pax1* in the development of the pharyngeal derivatives and pouches in medaka.

Reiterative endoderm expression of *pax1* in the segmental development of pouches

Compared with segmentation of the somitic mesoderm and hindbrain, there is little information about segmentation of the pharyngeal arches (Graham et al., 2014; Choe and Crump, 2015). Even though previous studies have underscored the importance of the endoderm and mesoderm for pharyngeal segmentation, there is limited information on how segmentation is brought about in the endoderm (Graham et al., 2005; Choe and Crump, 2015). In this study, we found that medaka *pax1* expression is activated reiteratively in cells where the next pouches will be formed. Additionally, we showed that endodermal *pax1* plays an indispensable role in segmental pouch formation, except for the first pouch and anterior wall of the second pouch. Importantly, *pax1* is required for the endodermal activation of *tbx1* and *fgf3* transcription, the functions of which in the development and patterning of endodermal pouches were described previously (Piotrowski et al., 2003; Crump et al., 2004; Herzog et al., 2004; Choe and Crump, 2014). The results of our TUNEL assay did not suggest an increase in apoptosis in the pharyngeal endoderm of the *pax1* mutants. The size of the pharyngeal endoderm in the wild-type and *pax1* mutant embryos did not differ significantly, suggesting that the loss of Pax1 does not cause developmental delay or loss of endoderm. These results indicate that *pax1* is required for primary reiteration in pharyngeal pouch segmentation.

How does *pax1* generate its reiterative expression pattern? The uniform pattern of *pax1* expression seen in the *pax1* mutant indicated that the reiterative pattern of *pax1* expression in the endoderm requires Pax1 function. The transcription of *pax1* is active throughout the pharyngeal endoderm in the absence of functional Pax1, suggesting that some form of negative regulation sets a *pax1*-negative region in the interpouch endoderm. In the vertebrate somite, Hes genes, which encode transcriptional repressors displaying an oscillatory expression pattern, play a role in the molecular clock through direct negative-feedback transcription loops (Hirata et al., 2002, 2004). Because Pax genes are basically transcription activators (Chalepakis et al., 1991; Noll, 1993), an indirect pathway might act to repress *pax1* transcription. In contrast to the transient expression of Hes genes in somites through cell-autonomous repression, *pax1* expression in pouches is retained after pouch segmentation and, therefore, repression of *pax1* may function in a non-cell-autonomous manner (Fig. 8).

Previous studies showed that Fgf and RA signaling pathways are required for pharyngeal pouch segmentation, and phenotypes associated with Fgf and RA deficiencies are similar to the *pax1* mutant phenotype in the endoderm (Wendling et al., 2000; Abu-Issa et al., 2002; Crump et al., 2004; Kopinke et al., 2006). In these previous studies, the expression patterns of *pax1/9* cognates were affected, corresponding to defects in the posterior pouches caused by the lack of RA (Wendling et al., 2000). Additionally, Tbx1 reportedly modulates the dynamics of RA signaling in the developing vertebrate head by regulating Cyp26 genes, which encode RA-degrading enzymes (Roberts et al., 2006; Bothe et al., 2011). Regarding the function of Fgf signaling in pouch formation, it has been shown that its inhibition causes complete loss of the pharyngeal pouches forming posterior to the second arch (Abu-Issa et al., 2002; Crump et al., 2004). Even though the complete picture remains obscure, our results highlight the novel role of *pax1* in activating the expression of *tbx1* and *fgf3*. Therefore, the role of *pax1* in pouch segmentation is probably tightly connected with the regulation of RA and Fgf signal transduction in the pharyngeal endoderm. Further investigations of the interplay and genetic relationships among relevant genes, including *pax1* and signaling pathway genes, will contribute to a deeper knowledge of the mechanism of pharyngeal segmentation.

Evolution of the mechanism of pharyngeal segmentation: from gill slits to pharyngeal arches

That *pax1* mutant medaka exhibit serious pouch defects is rather surprising, given that *Pax1* knockout mice reportedly show minimal defects in pharyngeal segmentation and, even in *Pax1;Pax9* double-homozygous mutant mice, no defects in pharyngeal segmentation have been reported (Su et al., 2001). This discrepancy in *Pax1* knockout phenotypes between mice and medaka might be due to evolutionary changes in the genetic hierarchy of *pax1/9* cognates,

Development (2016) 143, 1800-1810 doi:10.1242/dev.130039

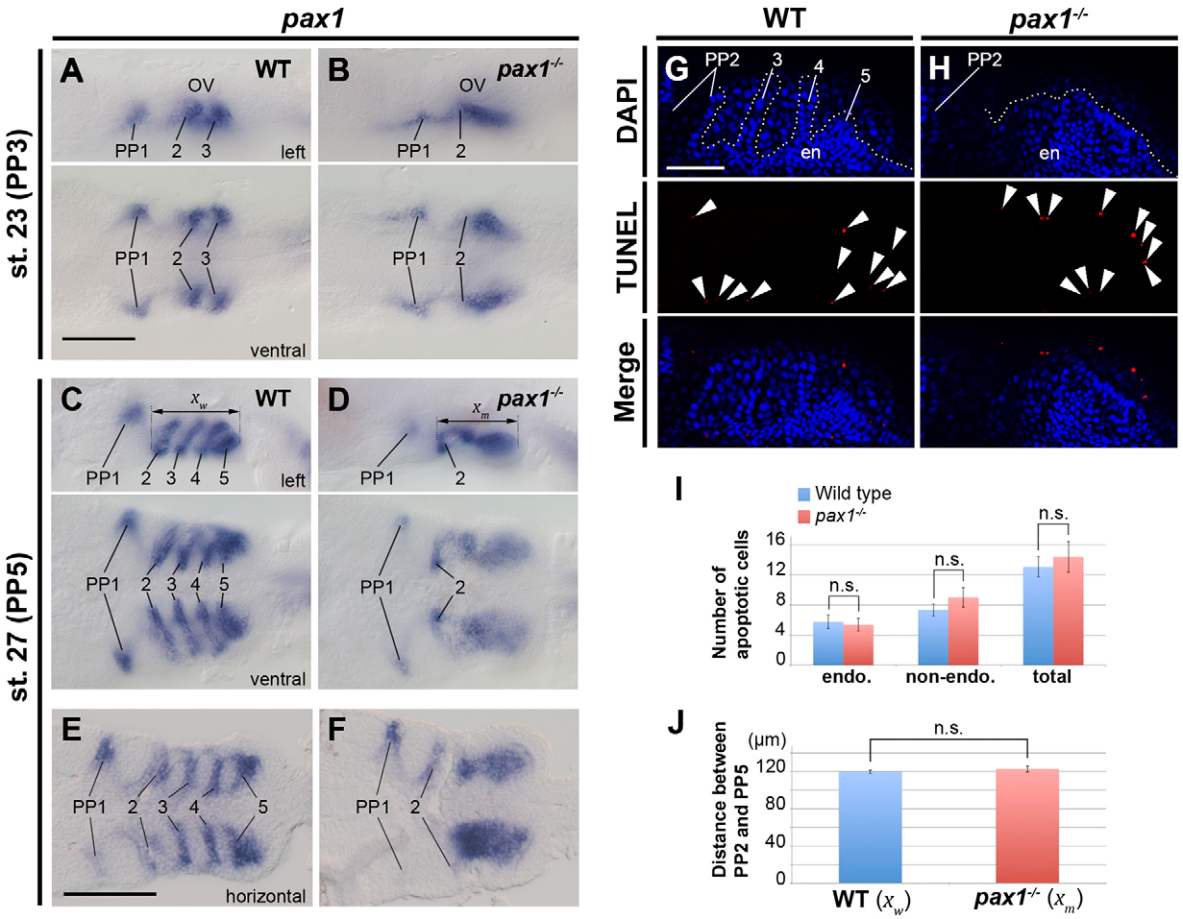

Fig. 7. Pax1 is required for the reiterative pattern of *pax1* expression in the pharyngeal endoderm. (A,B) Expression pattern of *pax1* in wild-type (A) and *pax1* mutant (B) embryos at stage 23. In *pax1* mutants, the reiterative pattern of *pax1* expression was disturbed, showing a continuous pattern posterior to PA2 (B, *n*=8). (C-F) Expression pattern of *pax1* in wild-type (C,E) and *pax1* mutant (D,F) embryos at stage 27. In *pax1* mutants, the reiterative *pax1* pattern observed in the wild-type embryos (C,E) was changed to a continuous pattern (D,F, *n*=9). (E,F) Horizontal sections of wild-type and *pax1* mutant embryos stained with *pax1* probe. (G,H) DAPI staining and TUNEL signals (arrowheads) in wild-type (G) and *pax1* mutant (H) embryos at stage 26. White dotted lines delineate endodermal regions. (I) Quantification of apoptotic cells (TUNEL signals) in the pharynx of wild-type (*n*=14) and *pax1* mutant (*n*=8) embryos in each region of the endoderm (endo, *P*=0.776), other regions (non-endo, *P*=0.297) and total (*P*=0.598) at stage 26. (J) Quantification of the size of the pharyngeal endoderm at stage 27. In wild type, the distance from the anterior epithelium of PP2 to the posterior epithelium of PP5 was measured (x_w, *n*=12). Because PP3-5 were not formed, the distance from the anterior epithelium of PP2 to the posterior limit of *pax1* expression was measured in *pax1* mutant embryos (x_m, *n*=9). x_w and x_m were not significantly different (*P*=0.413). Data represent mean±s.e.m. OV, otic vesicle; PP, pharyngeal pouch; en, endoderm; n.s., not significant. Scale bars: 100 μm in A-F; 50 μm in G,H.

tbx1, and other genes, and as such might constitute an example of developmental system drift (True and Haag, 2001). Previous studies in mouse reported that *Pax1/Pax9* regulate later organogenesis, such as that of the thymus and parathyroid gland, and palate skeletogenesis, rather than pouch segmentation (Peters et al., 1998, 1999; Su et al., 2001). The evolution of the pharyngeal derivatives seems to be closely related to adaptation to a terrestrial lifestyle. During vertebrate evolution, degeneration of the posterior gill skeleton and a reduction in pouch number are evident, and a pouch-derived parathyroid gland would be necessary for control of calcium homeostasis in the terrestrial as opposed to aquatic environment (Okabe and Graham, 2004; Graham and Richardson, 2012).

Regarding the function of *Pax1*/*Pax9* in pouch development in mice, one can consider the functional transition of *Pax1*/*Pax9* from segmentation to later organogenesis, such as that of the thymus. Accompanying such functional transition, alternative factors might have been recruited to the pouch segmentation regulatory network. *Ripply3*, which encodes a repressor of Tbx1, is a conceivable candidate, as this gene is expressed in the mouse pharyngeal endoderm in a similar fashion to medaka *pax1*, and its function is necessary for the segmentation of the third and posterior pouches (Okubo et al., 2011). Interestingly, the pouch defects that we found in *pax1* mutant medaka are almost identical to those seen in *Ripply3* mutant mice. We could not identify the sequence of *ripply3* in the whole-genome databases of medaka (Kasahara et al., 2007), stickleback (Jones et al., 2012), cod (Star et al., 2011), platyfish (Schartl et al., 2013), tilapia (http://ensembl.org/Oreochromis_niloticus/Info/Index), Amazon molly (http://ensembl.org/Poecilia_formosa/Info/Index) or puffer fish (Aparicio et al., 2002). In medaka, only one Ripply gene, annotated as *ripply2*, was found in the genome, but its expression was detected in paraxial mesoderm and not the pharynx (Fig. S6). However, we found a *ripply3* gene in the genome of the following fish species: coelacanth (Amemiya et al., 2013), spotted gar (http://ensembl.org/Lepisosteus_oculatus/Info/Index), cavefish (McGaugh et al., 2014), rainbow trout (Berthelot et al., 2014) and zebrafish (Kettleborough et al., 2013). Considering the phylogenetic relationships among fish species (Near et al., 2012), loss of the *ripply3* gene is likely to have occurred

Development (2016) 143, 1800-1810 doi:10.1242/dev.130039

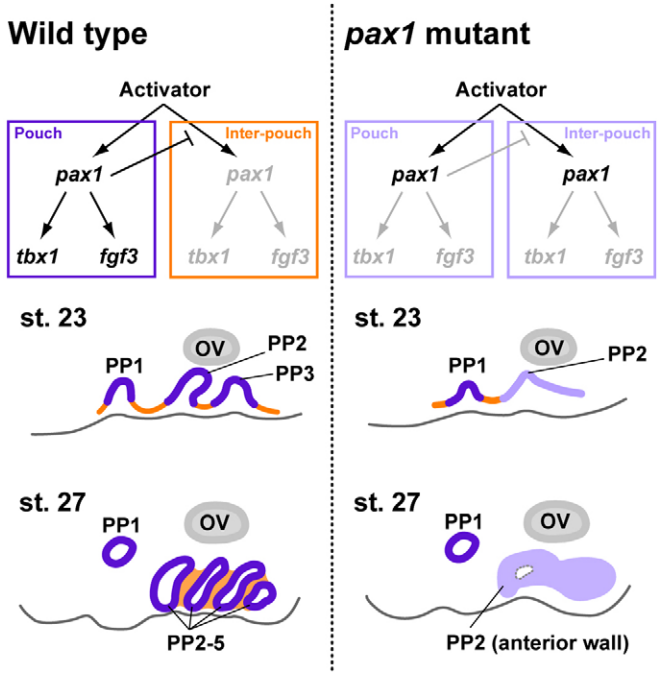

Fig. 8. Model of the genetic networks regulating pouch segmentation. In wild-type embryos, functional Pax1 specifically activates *tbx1* and *fgf3* expression in the pharyngeal pouches (purple). Downstream targets of Pax1 inhibit *pax1* transcription to create the interpouch endodermal regions (orange) in a non-cell-autonomous manner. Reiteration of these bifacial (*pax1*$^{+}$/*pax1*$^{-}$) endoderm patterns gives rise to the segmental pharyngeal pouches. In *pax1* mutants, negative regulation of *pax1* expression by Pax1 has no effect (pale purple). This results in no endodermal expression of *tbx1* and *fgf3* and continuous expression of *pax1* in the posterior pharynx, whereas expression in PP1 and the anterior wall of PP2 is almost normal. OV, otic vesicle; PP, pharyngeal pouch.

once among the common ancestors of the Neoteleostei clade. Although the function of teleost *ripply3* in pharyngeal segmentation is intriguing, surprisingly we did not find any abnormalities in pharyngeal segmentation in *ripply3*$^{-/-}$ zebrafish generated by TALEN-mediated mutagenesis (our unpublished data). In contrast to the highly conserved morphologies of vertebrate pharyngeal arches, our study reveals a striking difference in pharyngeal pouch segmentation between mammals and teleosts, serving as an additional example of developmental system drift. Careful analyses in each animal system will be required in order to obtain a more comprehensive understanding of vertebrate pharyngeal development.

The original function of *pax1/9* might be related to gill slit segmentation itself, as evidenced by the highly conserved expression patterns of the cognates in deuterostome pharyngeal endoderm (Holland et al., 1995; Müller et al., 1996; Wallin et al., 1996; Ogasawara et al., 1999, 2000; Lowe et al., 2003; Gillis et al., 2012). Recent *pax1/9* knockdown experiments in amphioxus revealed a role in gill slit segmentation and that *pax1/9* deficiency leads to a reduction in *tbx1/10* expression (Liu et al., 2015). The present study shows that the genetic regulation of *pax1* and *tbx1* and the function of *pax1* in gill slit segmentation are conserved among aquatic chordates. Furthermore, our model provides a reasonable explanation for gill slit development in hemichordates, which lack *tbx1/10* expression in the pharynx (Gillis et al., 2012). Regarding the origin of the deuterostome gill slit, *pax1/9* might have acquired a reiterative expression pattern in the pharyngeal endoderm, which may then have facilitated the segmental development of endodermal outpocketings. Subsequently, *tbx1/10* might have participated in pharyngeal segmentation under the control of *pax1* in the common ancestors of chordates.

MATERIALS AND METHODS

Medaka

Mature adult wild-type medaka were kept in fresh water in plastic aquaria under artificial reproductive conditions (10 h dark, 14 h light; 26°C). Developmental stages were determined as previously outlined (Iwamatsu, 2004). This study was performed in accordance with the Guidelines for Animal Experimentation of the National Institutes of Natural Sciences, with approval of the Institutional Animal Care and Use Committee of the National Institutes of Natural Sciences.

TALEN-mediated mutagenesis of *pax1* and morpholino knockdown

The medaka *pax1* mutant was established using the TALEN method (Joung and Sander, 2013). The TALENs were designed in the paired domain of the *pax1* gene and constructed as previously reported (Ansai et al., 2014). A medaka *pax1* mutant with a 7 bp deletion in the paired domain was obtained. Details of TALEN-mediated mutagenesis of *pax1* and fish genotyping are shown in Fig. S1. The *pax1* and control morpholinos are described in the supplementary Materials and Methods.

Staining

Whole-mount skeletal staining with Alcian Blue (Sigma, A5268) was performed using a modified protocol (Yasutake et al., 2004). Details are provided in the supplementary Materials and Methods.

Whole-mount immunostaining of medaka embryos was performed as previously described (Sakai et al., 2007). Neural axons were visualized using an anti-acetylated tubulin monoclonal antibody (Sigma, T6793; 1:800) and Alexa 546 rabbit anti-mouse IgG secondary antibody (ThermoFisher, A-11060; 1:600). Images were acquired using a TCS SP8 inverted confocal laser scanning microscope (Leica).

Whole-mount *in situ* hybridization was performed as previously described (Yasutake et al., 2004). In double-fluorescence *in situ* hybridization experiments, anti-DIG-POD (Roche) and anti-FITC-POD (Dako) were used to detect each hapten in RNA probes. Fluorescent signals were detected with a TSA Plus Cy3/fluorescein system (PerkinElmer). Primers for gene cloning are listed in Table S1. The probes for *pax1* and *pax9* were reported previously (Mise et al., 2008). The plasmid encoding *foxN1* was provided by Dr Norimasa Iwanami (Li et al., 2007). Gene expression patterns were examined by observing whole-mount specimens or cryostat sections.

TUNEL assay

The mean number of apoptotic cells, as determined by TUNEL assay, in the pharyngeal region was calculated and subject to statistical analysis as detailed in the supplementary Materials and Methods.

Acknowledgements

We thank Drs N. Iwanami and Y. Takahama for providing the *foxN1* plasmid; Drs T. Nishimura and M. Tanaka and Ms M. Kikuchi for providing wild-type medaka embryos and for technical support; Ms H. Utsumi for technical support; the Spectrography and Bioimaging Facility, NIBB Core Research Facilities, for technical support; Mrs S. Ukai for assistant secretary support; and all members of the H.W. and S.T. laboratories for helpful discussions.

Competing interests

The authors declare no competing or financial interests.

Author contributions

K.O. and H.W. conceived of and designed the research; K.O., K.I. and T.M. undertook the experiments and K.O. confirmed and analyzed the data; K.I. and A.K. generated *pax1* mutant medaka by TALEN; K.O., S.T. and H.W. wrote and edited the manuscript.

Funding

This work was supported by Grants-in-Aid for Japan Society for the Promotion of Science (JSPS) Fellows to K.O. [no. 11J00382], for Scientific Research on

Innovative Areas to S.T. [no. 24111002] and for Scientific Research on Innovative Areas to H.W. [no. 23128502].

Supplementary information

Supplementary information available online at
http://dev.biologists.org/lookup/suppl/doi:10.1242/dev.130039/-/DC1

References

Abu-Issa, R., Smyth, G., Smoak, I., Yamamura, K. and Meyers, E. N. (2002). *Fgf8* is required for pharyngeal arch and cardiovascular development in the mouse. *Development* **129**, 4613-4625.

Amemiya, C. T., Alföldi, J., Lee, A. P., Fan, S., Philippe, H., MacCallum, I., Braasch, I., Manousaki, T., Schneider, I., Rohner, N. et al. (2013). The African coelacanth genome provides insights into tetrapod evolution. *Nature* **496**, 311-316.

Ansai, S., Inohaya, K., Yoshiura, Y., Schartl, M., Uemura, N., Takahashi, R. and Kinoshita, M. (2014). Design, evaluation, and screening methods for efficient targeted mutagenesis with transcription activator-like effector nucleases in medaka. *Dev. Growth Differ.* **56**, 98-107.

Aparicio, S., Chapman, J., Stupka, E., Putnam, N., Chia, J.-M., Dehal, P., Christoffels, A., Rash, S., Hoon, S., Smit, A. et al. (2002). Whole-genome shotgun assembly and analysis of the genome of *Fugu rubripes*. *Science* **297**, 1301-1310.

Berthelot, C., Brunet, F., Chalopin, D., Juanchich, A., Bernard, M., Noël, B., Bento, P., Da Silva, C., Labadie, K., Alberti, A. et al. (2014). The rainbow trout genome provides novel insights into evolution after whole-genome duplication in vertebrates. *Nat. Commun.* **5**, 3657.

Bothe, I., Tenin, G., Oseni, A. and Dietrich, S. (2011). Dynamic control of head mesoderm patterning. *Development* **138**, 2807-2821.

Chalepakis, G., Fritsch, R., Fickenscher, H., Deutsch, U., Goulding, M. and Gruss, P. (1991). The molecular basis of the *undulated*/*Pax-1* mutation. *Cell* **66**, 873-884.

Chapman, D. L., Garvey, N., Hancock, S., Alexiou, M., Agulnik, S. I., Gibson-Brown, J. J., Cebra-Thomas, J., Bollag, R. J., Silver, L. M. and Papaioannou, V. E. (1996). Expression of the T-box family genes, *Tbx1-Tbx5*, during early mouse development. *Dev. Dyn.* **206**, 379-390.

Choe, C. P. and Crump, J. G. (2014). Tbx1 controls the morphogenesis of pharyngeal pouch epithelia through mesodermal Wnt11r and Fgf8a. *Development* **141**, 3583-3593.

Choe, C. P. and Crump, J. G. (2015). Dynamic epithelia of the developing vertebrate face. *Curr. Opin. Genet. Dev.* **32**, 66-72.

Choe, C. P., Collazo, A., Trinh, L. A., Pan, L., Moens, C. B. and Crump, J. G. (2013). Wnt-dependent epithelial transitions drive pharyngeal pouch formation. *Dev. Cell* **24**, 296-309.

Clausen, S. and Smith, A. B. (2005). Palaeoanatomy and biological affinities of a Cambrian deuterostome (Stylophora). *Nature* **438**, 351-354.

Crump, J. G., Maves, L., Lawson, N. D., Weinstein, B. M. and Kimmel, C. B. (2004). An essential role for Fgfs in endodermal pouch formation influences later craniofacial skeletal patterning. *Development* **131**, 5703-5716.

David, N. B., Saint-Etienne, L., Tsang, M., Schilling, T. F. and Rosa, F. M. (2002). Requirement for endoderm and FGF3 in ventral head skeleton formation. *Development* **129**, 4457-4468.

Gillis, J. A., Fritzenwanker, J. H. and Lowe, C. J. (2012). A stem-deuterostome origin of the vertebrate pharyngeal transcriptional network. *Proc. Biol. Sci. B Biol. Sci.* **279**, 237-246.

Graham, A. and Richardson, J. (2012). Developmental and evolutionary origins of the pharyngeal apparatus. *EvoDevo* **3**, 24.

Graham, A., Okabe, M. and Quinlan, R. (2005). The role of the endoderm in the development and evolution of the pharyngeal arches. *J. Anat.* **207**, 479-487.

Graham, A., Butts, T., Lumsden, A. and Kiecker, C. (2014). What can vertebrates tell us about segmentation? *EvoDevo* **5**, 24.

Herzog, W., Sonntag, C., von der Hardt, S., Roehl, H. H., Varga, Z. M. and Hammerschmidt, M. (2004). Fgf3 signaling from the ventral diencephalon is required for early specification and subsequent survival of the zebrafish adenohypophysis. *Development* **131**, 3681-3692.

Hirata, H., Yoshiura, S., Ohtsuka, T., Bessho, Y., Harada, T., Yoshikawa, K. and Kageyama, R. (2002). Oscillatory expression of the bHLH factor Hes1 regulated by a negative feedback loop. *Science* **298**, 840-843.

Hirata, H., Bessho, Y., Kokubu, H., Masamizu, Y., Yamada, S., Lewis, J. and Kageyama, R. (2004). Instability of Hes7 protein is crucial for the somite segmentation clock. *Nat. Genet.* **36**, 750-754.

Holland, N., Holland, L. and Kozmik, Z. (1995). An amphioxus *Pax* gene, *AmphiPax-1*, expressed in embryonic endoderm, but not in mesoderm: implications for the evolution of class I paired box genes. *Mol. Mar. Biol. Biotechnol.* **4**, 206-214.

Iwamatsu, T. (2004). Stages of normal development in the medaka *Oryzias latipes*. *Mech. Dev* **121**, 605-618.

Jandzik, D., Hawkins, M. B., Cattell, M. V., Cerny, R., Square, T. A. and Medeiros, D. M. (2014). Roles for FGF in lamprey pharyngeal pouch formation and skeletogenesis highlight ancestral functions in the vertebrate head. *Development* **141**, 629-638.

Jerome, L. A. and Papaioannou, V. E. (2001). DiGeorge syndrome phenotype in mice mutant for the T-box gene, *Tbx1*. *Nat. Genet.* **27**, 286-291.

Jones, F. C., Grabherr, M. G., Chan, Y. F., Russell, P., Mauceli, E., Johnson, J., Swofford, R., Pirun, M., Zody, M. C., White, S. et al. (2012). The genomic basis of adaptive evolution in threespine sticklebacks. *Nature* **484**, 55-61.

Joung, J. K. and Sander, J. D. (2013). TALENs: a widely applicable technology for targeted genome editing. *Nat. Rev. Mol. Cell Biol.* **14**, 49-55.

Kasahara, M., Naruse, K., Sasaki, S., Nakatani, Y., Qu, W., Ahsan, B., Yamada, T., Nagayasu, Y., Doi, K., Kasai, Y. et al. (2007). The medaka draft genome and insights into vertebrate genome evolution. *Nature* **447**, 714-719.

Kettleborough, R. N. W., Busch-Nentwich, E. M., Harvey, S. A., Dooley, C. M., de Bruijn, E., van Eeden, F., Sealy, I., White, R. J., Herd, C., Nijman, I. J. et al. (2013). A systematic genome-wide analysis of zebrafish protein-coding gene function. *Nature* **496**, 494-497.

Kopinke, D., Sasine, J., Swift, J., Stephens, W. Z. and Piotrowski, T. (2006). Retinoic acid is required for endodermal pouch morphogenesis and not for pharyngeal endoderm specification. *Dev. Dyn.* **235**, 2695-2709.

Kuratani, S., Ueki, T., Hirano, S. and Aizawa, S. (1998). Rostral truncation of a cyclostome, *Lampetra japonica*, induced by all-*trans* retinoic acid defines the head/trunk interface of the vertebrate body. *Dev. Dyn.* **211**, 35-51.

Lee, K.-H., Xu, Q. and Breitbart, R. E. (1996). A new tinman-related gene, *nkx2.7*, anticipates the expression of *nkx2.5* and *nkx2.3* in zebrafish heart and pharyngeal endoderm. *Dev. Biol.* **180**, 722-731.

Lee, G.-H., Chang, M.-Y., Hsu, C.-H. and Chen, Y.-H. (2011). Essential roles of basic helix-loop-helix transcription factors, Capsulin and Musculin, during craniofacial myogenesis of zebrafish. *Cell. Mol. Life Sci.* **68**, 4065-4078.

Li, J., Iwanami, N., Hoa, V. Q., Furutani-Seiki, M. and Takahama, Y. (2007). Noninvasive intravital imaging of thymocyte dynamics in medaka. *J. Immunol.* **179**, 1605-1615.

Liu, X., Li, G., Liu, X. and Wang, Y.-Q. (2015). The role of the *Pax1/9* gene in the early development of amphioxus pharyngeal gill slits. *J. Exp. Zool. B Mol. Dev. Evol.* **324**, 30-40.

Lowe, C. J., Wu, M., Salic, A., Evans, L., Lander, E., Stange-Thomann, N., Gruber, C. E., Gerhart, J. and Kirschner, M. (2003). Anteroposterior patterning in hemichordates and the origins of the chordate nervous system. *Cell* **113**, 853-865.

McGaugh, S. E., Gross, J. B., Aken, B., Blin, M., Borowsky, R., Chalopin, D., Hinaux, H., Jeffery, W. R., Keene, A., Ma, L. et al. (2014). The cavefish genome reveals candidate genes for eye loss. *Nat. Commun.* **5**, 5307.

Mise, T., Iijima, M., Inohaya, K., Kudo, A. and Wada, H. (2008). Function of *Pax1* and *Pax9* in the sclerotome of medaka fish. *Genesis* **46**, 185-192.

Müller, T. S., Ebensperger, C., Neubüser, A., Koseki, H., Balling, R., Christ, B. and Wilting, J. (1996). Expression of avian *Pax1* and *Pax9* is intrinsically regulated in the pharyngeal endoderm, but depends on environmental influences in the paraxial mesoderm. *Dev. Biol.* **178**, 403-417.

Near, T. J., Eytan, R. I., Dornburg, A., Kuhn, K. L., Moore, J. A., Davis, M. P., Wainwright, P. C., Friedman, M. and Smith, W. L. (2012). Resolution of ray-finned fish phylogeny and timing of diversification. *Proc. Natl. Acad. Sci. USA* **109**, 13698-13703.

Nechiporuk, A., Linbo, T. and Raible, D. W. (2005). Endoderm-derived Fgf3 is necessary and sufficient for inducing neurogenesis in the epibranchial placodes in zebrafish. *Development* **132**, 3717-3730.

Noden, D. M. (1988). Interactions and fates of avian craniofacial mesenchyme. *Development* **103** Suppl., 121-140.

Noll, M. (1993). Evolution and role of *Pax* genes. *Curr. Opin. Genet. Dev.* **3**, 595-605.

Ogasawara, M., Wada, H., Peters, H. and Satoh, N. (1999). Developmental expression of *Pax1/9* genes in urochordate and hemichordate gills: insight into function and evolution of the pharyngeal epithelium. *Development* **126**, 2539-2550.

Ogasawara, M., Shigetani, Y., Hirano, S., Satoh, N. and Kuratani, S. (2000). *Pax1*/*Pax9*-Related genes in an agnathan vertebrate, *Lampetra japonica*: expression pattern of *LjPax9* implies sequential evolutionary events toward the gnathostome body plan. *Dev. Biol.* **223**, 399-410.

Okabe, M. and Graham, A. (2004). The origin of the parathyroid gland. *Proc. Natl. Acad. Sci. USA* **101**, 17716-17719.

Okubo, T., Kawamura, A., Takahashi, J., Yagi, H., Morishima, M., Matsuoka, R. and Takada, S. (2011). Ripply3, a Tbx1 repressor, is required for development of the pharyngeal apparatus and its derivatives in mice. *Development* **138**, 339-348.

Peters, H., Neubüser, A., Kratochwil, K. and Balling, R. (1998). *Pax9*-deficient mice lack pharyngeal pouch derivatives and teeth and exhibit craniofacial and limb abnormalities. *Genes Dev.* **12**, 2735-2747.

Development (2016) 143, 1800-1810 doi:10.1242/dev.130039

Peters, H., Wilm, B., Sakai, N., Imai, K., Maas, R. and Balling, R. (1999). Pax1 and Pax9 synergistically regulate vertebral column development. *Development* **126**, 5399-5408.

Piotrowski, T., Ahn, D.-G., Schilling, T. F., Nair, S., Ruvinsky, I., Geisler, R., Rauch, G.-J., Haffter, P., Zon, L. I., Zhou, Y. et al. (2003). The zebrafish *van gogh* mutation disrupts *tbx1*, which is involved in the DiGeorge deletion syndrome in humans. *Development* **130**, 5043-5052.

Quinlan, R., Gale, E., Maden, M. and Graham, A. (2002). Deficits in the posterior pharyngeal endoderm in the absence of retinoids. *Dev. Dyn.* **225**, 54-60.

Roberts, C., Ivins, S., Cook, A. C., Baldini, A. and Scambler, P. J. (2006). *Cyp26* genes *a1*, *b1* and *c1* are down-regulated in *Tbx1* null mice and inhibition of Cyp26 enzyme function produces a phenocopy of DiGeorge Syndrome in the chick. *Hum. Mol. Genet.* **15**, 3394-3410.

Sakai, C., Konno, F., Nakano, O., Iwai, T., Yokota, T., Lee, J., Nishida-Umehara, C., Kuroiwa, A., Matsuda, Y. and Yamashita, M. (2007). Chromosome elimination in the interspecific hybrid medaka between *Oryzias latipes* and *O.* hubbsi. *Chromosome Res.* **15**, 697-709.

Schartl, M., Walter, R. B., Shen, Y., Garcia, T., Catchen, J., Amores, A., Braasch, I., Chalopin, D., Volff, J. N., Lesch, K. P. et al. (2013). The genome of the platyfish, Xiphophorus maculatus, provides insights into evolutionary adaptation and several complex traits. *Nat. Genet.* **45**, 567-572.

Star, B., Nederbragt, A. J., Jentoft, S., Grimholt, U., Malmstrøm, M., Gregers, T. F., Rounge, T. B., Paulsen, J., Solbakken, M. H., Sharma, A. et al. (2011). The genome sequence of Atlantic cod reveals a unique immune system. *Nature* **477**, 207-210.

Su, D.-M., Ellis, S., Napier, A., Lee, K. and Manley, N. R. (2001). *Hoxa3* and *pax1* regulate epithelial cell death and proliferation during thymus and parathyroid organogenesis. *Dev. Biol.* **236**, 316-329.

True, J. R. and Haag, E. S. (2001). Developmental system drift and flexibility in evolutionary trajectories. *Evol. Dev.* **3**, 109-119.

Veitch, E., Begbie, J., Schilling, T. F., Smith, M. M. and Graham, A. (1999). Pharyngeal arch patterning in the absence of neural crest. *Curr. Biol.* **9**, 1481-1484.

Vitelli, F., Morishima, M., Taddei, I., Lindsay, E. A. and Baldini, A. (2002). *Tbx1* mutation causes multiple cardiovascular defects and disrupts neural crest and cranial nerve migratory pathways. *Hum. Mol. Genet.* **11**, 915-922.

Wallin, J., Eibel, H., Neubuser, A., Wilting, J., Koseki, H. and Balling, R. (1996). *Pax1* is expressed during development of the thymus epithelium and is required for normal T-cell maturation. *Development* **122**, 23-30.

Wendling, O., Dennefeld, C., Chambon, P. and Mark, M. (2000). Retinoid signaling is essential for patterning the endoderm of the third and fourth pharyngeal arches. *Development* **127**, 1553-1562.

Xu, H., Cerrato, F. and Baldini, A. (2005). Timed mutation and cell-fate mapping reveal reiterated roles of *Tbx1* during embryogenesis, and a crucial function during segmentation of the pharyngeal system via regulation of endoderm expansion. *Development* **132**, 4387-4395.

Yasutake, J., Inohaya, K. and Kudo, A. (2004). Twist functions in vertebral column formation in medaka, *Oryzias latipes*. *Mech. Dev.* **121**, 883-894.

Zhang, Z., Huynh, T. and Baldini, A. (2006). Mesodermal expression of *Tbx1* is necessary and sufficient for pharyngeal arch and cardiac outflow tract development. *Development* **133**, 3587-3595.

Zou, D., Silvius, D., Davenport, J., Grifone, R., Maire, P. and Xu, P.-X. (2006). Patterning of the third pharyngeal pouch into thymus/parathyroid by Six and Eya1. *Dev. Biol.* **293**, 499-512.

Supplementary Materials and Methods

Morpholino knockdown

Morpholino antisense oligonucleotide (MO) was purchased from Gene Tools. The target of *pax1*-MO (5'-CCT CTC CAT AGG TTT GCT CCA TTT G-3') was the sequence at the translation start site of *pax1* mRNA (Mise et al., 2008). As a control experiment, Standard Control MO (5'-CCT CTT ACC TCA GTT ACA ATT TAT A-3') was used, as recommended by Gene Tools. These MOs were dissolved in RNase-free water to a final concentration of 0.5 mM and injected into one-cell-stage embryos.

Skeletal staining

For the visualization of cartilage structures, larvae at 2 days after hatching were fixed overnight in 4% paraformaldehyde at 4°C and then washed two times in phosphate-buffered saline containing 0.1% Tween-20 (PBST). The larvae were stained overnight in alcian blue solution (10% alcian blue, 65% ethanol, 25% glacial acetic acid). After gradual transfer to PBST through an ethanol series, the specimens were bleached with hydrogen peroxide (3% hydrogen peroxide, 1% potassium hydroxide) for 2 hours and washed two times in PBST. Next, the larvae were treated with 1% trypsin in a saturated 30% sodium borate solution at room temperature for 3 hours. Stained larvae were gradually transferred to glycerol. The pharyngeal cartilages were dissected for observation using fine forceps.

TUNEL assay, measurement of the pharynx size and statistics

Apoptotic cells were examined by TUNEL assay. Embryos were fixed with 4% paraformaldehyde overnight at 4°C and then washed three times in PBST. Manually dechorionized embryos were dehydrated with methanol at –20°C. After gradual rehydration, the embryos were permeabilized with 10 µg/ml of proteinase K for 20 minutes at room temperature, followed by 4% paraformaldehyde. After three washes with PBST, the embryos were incubated with 18 µl of labeling solution plus 2 µl of enzyme solution (In Situ Cell Death Detection Kit-TMR Red, Roche) at room temperature for 3 hours. Subsequently, the embryos were washed with PBST three times and stained with DAPI to visualize nuclei and define the endodermal

morphologies. Stained embryos were scanned on an AXIO Imager Z1 with ApoTome (Zeiss). Horizontal Z sections of 1.4-μm thickness, representing a central cross section of the gut tube, were obtained. Within the Z sections, all TUNEL signals distributed in the pharyngeal region posterior to the second arch were counted. The lengths of the pharyngeal regions, from the second pouch to the fifth pouch (in wild type) or the second pouch to the posterior end of the *pax1*-positive endoderm (in *pax1* mutant), were measured on an AXIO Imager Z1 with AxioVision (Zeiss). The mean number of TUNEL-positive cells and mean length of the pharyngeal region were calculated and graphed in Microsoft Excel. Significance was evaluated by a two-tailed Student's *t*-test. Data are presented as mean ± s.e.m., and differences were considered significant at $P < 0.05$.

Mise, T., Iijima, M., Inohaya, K., Kudo, A. and Wada, H. (2008). Function of *Pax1* and *Pax9* in the sclerotome of medaka fish. *Genesis* **46**, 185-192.

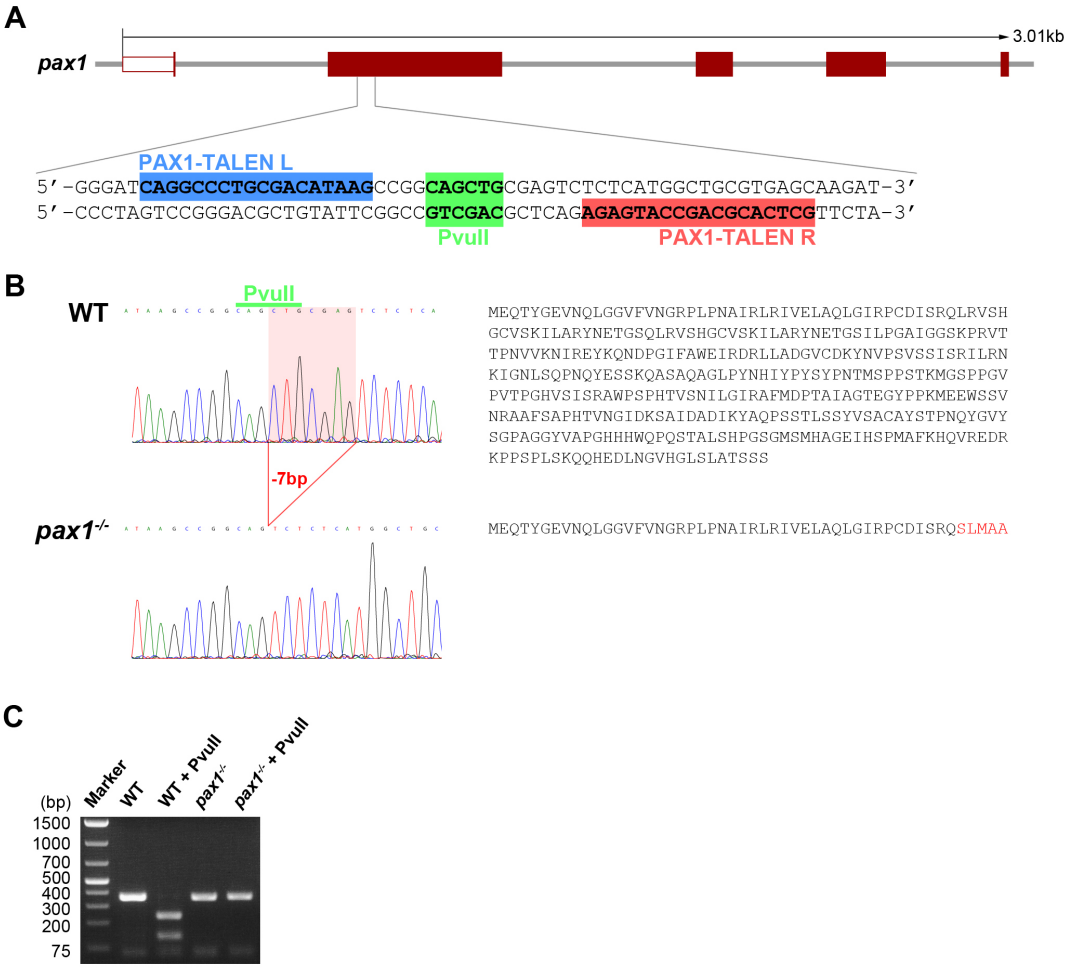

Figure S1. Generation of *pax1* mutants by TALEN.

(A) Schematic representation of the genomic structure of the medaka *pax1* gene and the TALEN target sites. A *Pvu*II restriction site (green) is flanked by the left (blue) and right (red) TALEN target sites in the second exon of *pax1*.

(B) A 7-bp deletion induced by TALEN resulted in significant truncation of the Pax1 protein. Sequencing analysis of the *pax1* mutant showed that the 7-bp deletion contained the *Pvu*II site. This frameshift mutation results in an abnormal amino acid sequence (red SLMAA) and a C-terminal truncation that includes a large part of the paired domain.

(C) Gel image of PCR products for *pax1* genotyping. A fragment of *pax1* was amplified from wild-type and *pax1*-mutant embryos and digested with *Pvu*II, which cleaves the wild-type allele but not the mutant allele. Sequences of the primers for the genotyping were 5’-AGC AAA CCT ATG GAG AGG TG-3’ and 5’-GCT GAT CGA ACT AAC AGA CG-3’.

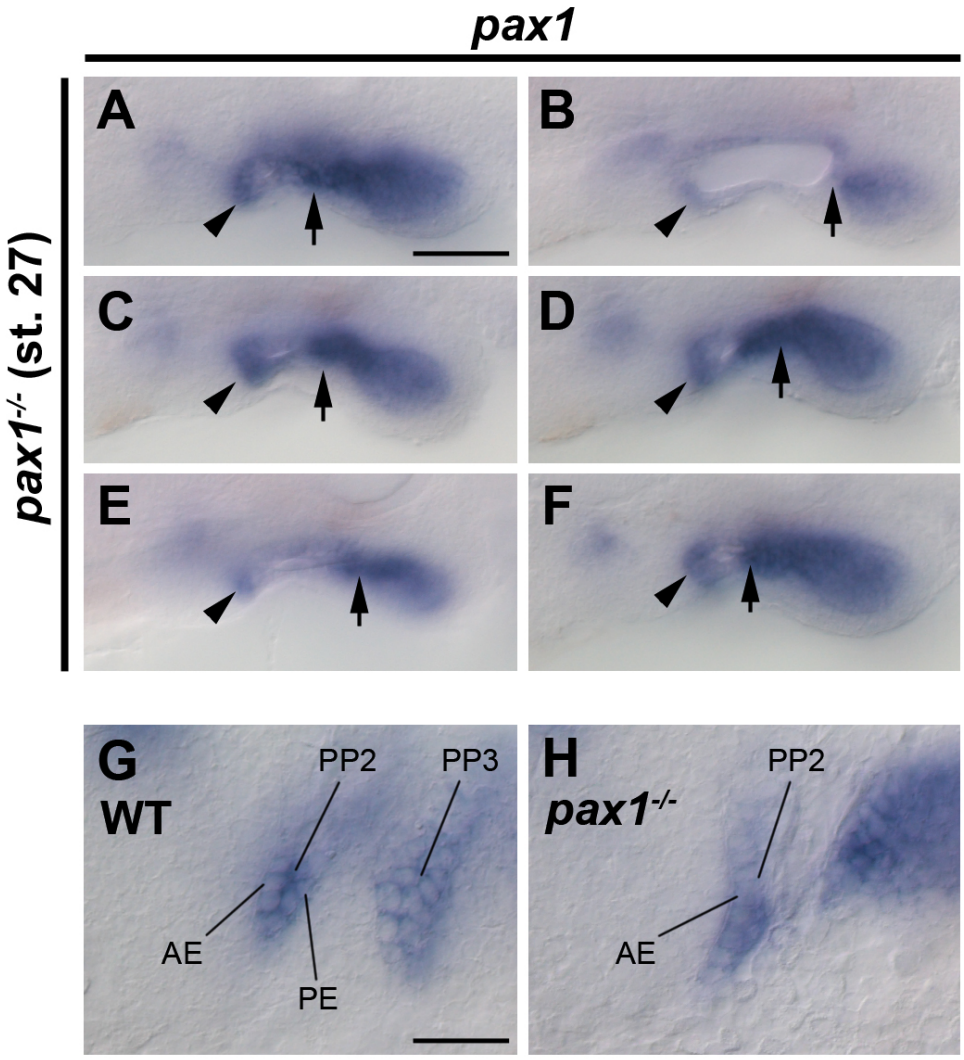

Figure S2. Second pharyngeal pouches in *pax1* mutants.

(A-F) Various morphologies of irregular slits forming posterior to the second arch. The pharyngeal endoderm of *pax1* mutants at stage 27 was visualized using *pax1* expression. Although the positions of the anterior walls of PP2 (arrowheads) were fixed in standard positions, those of the posterior ends of slit openings (arrows) were irregularly set in the mutants.

(G, H) High-magnification flat-mount images focused around PP2 at stage 27. The pharyngeal pouches or endodermal cells were visualized using *pax1* expression. Normally, PP2 (as well as other pouches) exhibited a bilayered morphology, composed of AE and PE. In *pax1* mutants, however, PP2 was composed of monolayer AE, and the PE structure was not found. PP, pharyngeal pouch; AE, anterior epithelium; PE, posterior epithelium. Scale bars, 50 μm in A-F, 25 μm in G and H.

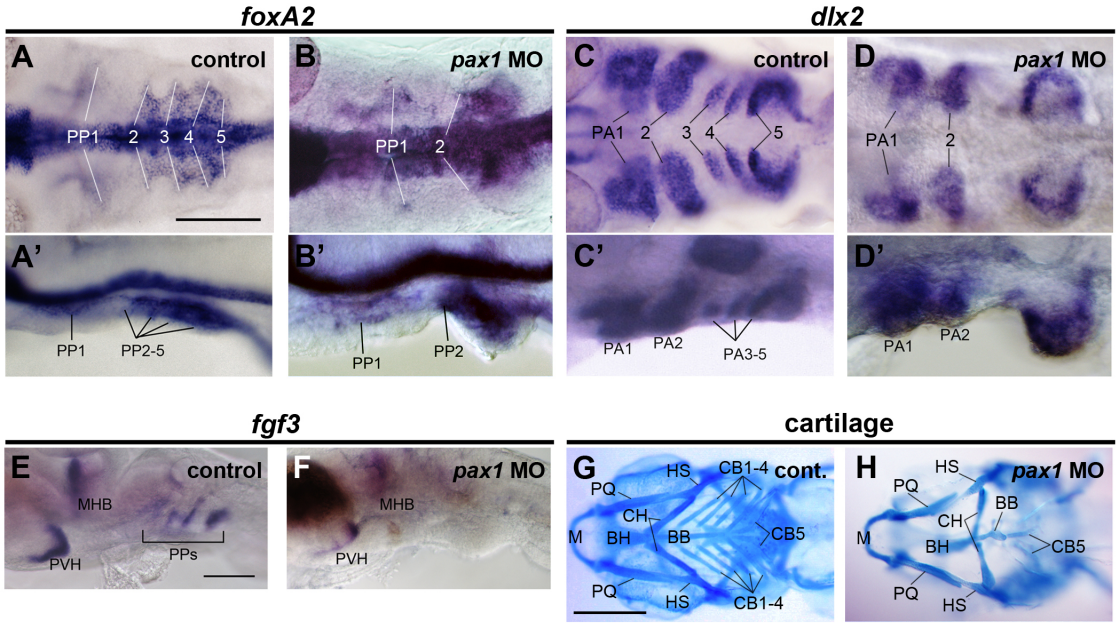

Figure S3. Phenocopy of *pax1* mutants by the *pax1*-specific morpholino.

(A-D) Expression of *foxA2* (A, A', B, B') and *dlx2* (C, C', D, D') was observed at stage 27 to reveal the distribution of neural crest cells and the endoderm, respectively. Whole-mount embryos were observed from the ventral (A-D) and left (A'-D') sides. In *pax1* morphants, although neural crest cells migrated to the ventral side, these cells were not divided into PA3-5 (n = 20/20, D, D') due to defects of PP3-5 (n = 24/27, B, B'), as seen in the *pax1*-mutant embryos.

(D, F) Expression of *fgf3* in control (E) and *pax1* morphant (F) embryos. The pharyngeal expression of *fgf3* was absent in the morphants (n = 8/8, F).

(G, H) Ventral whole-mount views showing alcian blue–stained pharyngeal cartilages of control (G) and *pax1*-morphant (H) larvae at 2 days after hatching. In *pax1* morphants, CB1-4 were lost (n = 18/25, H).

MHB, mid-hindbrain boundary; PA, pharyngeal arch; PP, pharyngeal pouch; PVH, paraventricular hypothalamic nucleus; BB, basibranchial; BH, basihyal; CB, ceratobranchial; CH, ceratohyal; HS, hyosymplectic; M, Meckel's; PQ, palatoquadrate. Scale bars; 100 μm in A and E, 250 μm in G.

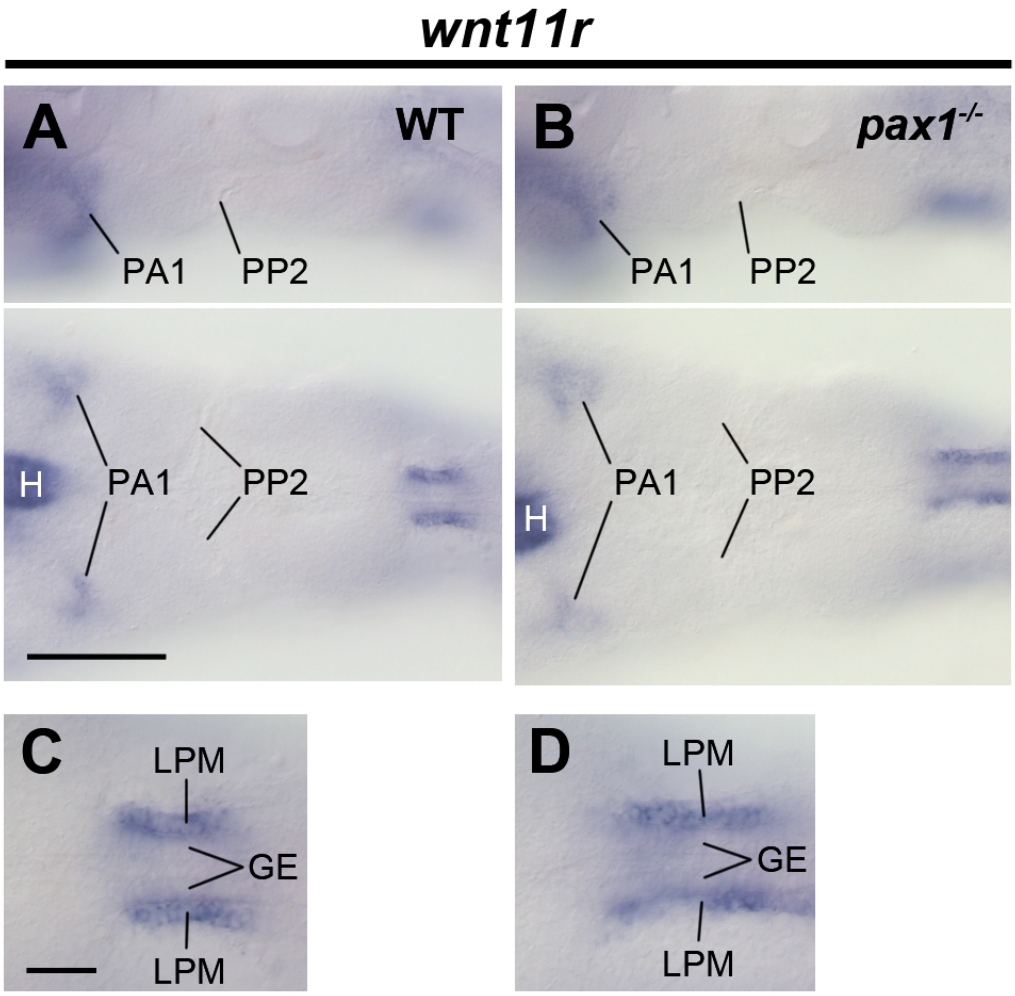

Figure S4. Expression pattern of *wnt11r* in medaka embryos at stage 27.

(A-D) Expression pattern of *wnt11r* in the pharynx of medaka at stage 27. In both wild-type and *pax1*-mutant embryos, *wnt11r* was not expressed in the pharyngeal mesoderm, except for PA1 (n = 19). Mesodermal expression was observed in the LPM surrounding the GE, just posterior to the pharynx, as shown by the high-magnification images of the boundary between the pharynx and the foregut (C, D). In A and B, upper and lower panels show left side and flat-mount views of the embryos, respectively. PA, pharyngeal arch; PP, pharyngeal pouch; LPM, lateral plate mesoderm; GE, gut endoderm. Scale bars: 100 μm in A and B, 25 μm in C and D.

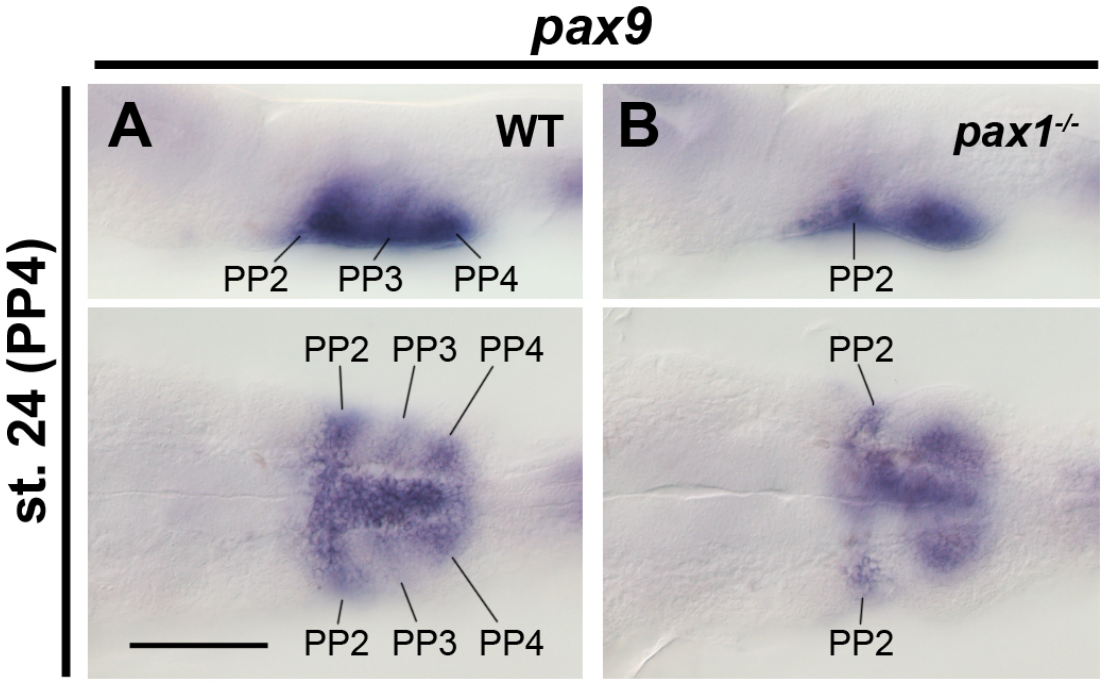

Figure S5. A wide range of *pax9* expression in pharyngeal endoderm.

(A, B) Expression pattern of *pax9* in the pharyngeal endoderm of wild-type (A) and *pax1*-mutant (B) embryos at stage 24. From medial to lateral, *pax9* was widely expressed in the pharyngeal endoderm posterior to the second arch. The *pax9* expression pattern was different from the pouch-specific pattern of *pax1* expression (A). In *pax1* mutants, although the third and fourth pouches were not formed, *pax9* was expressed in the pharyngeal endoderm posterior to the second arch (n = 16, B).

PP, pharyngeal pouch. Scale bar; 100 μm in A.

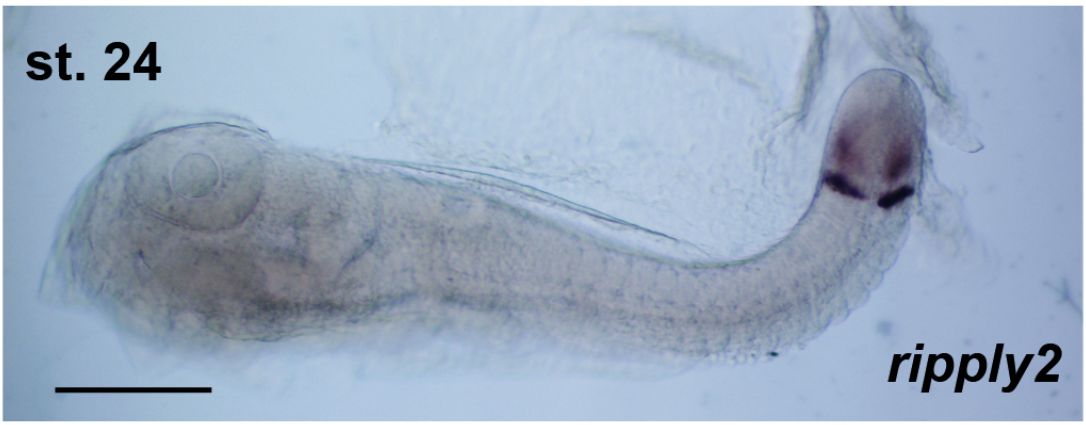

Figure S6. Expression pattern of *ripply2* in the medaka embryo.

The only *ripply* gene in the medaka genome is *ripply2*. At stage 24, expression of *ripply2* was detected in the presomitic mesoderm and in the posterior somites, but not in the pharyngeal region. Scale bar: 200 μm.

Supplementary Tables

Table S1. The list of primers for PCR to amplify cDNA fragments of genes

Gene	Forward primer sequence	Reverse primer sequence
dlx2	5'- GAA CCT AAA CAC CGA TAT GCA TTC CAA CCA -3'	5'- CTA AAA TAT CGT CCC GGC GCT TAT TGC AG -3'
fgf3	5'- CGC TCA GCA TTC ACA CTT TGG ATG G -3'	5'- GCC TCT CTC TTC CTG CCT CGC TTG C -3'
foxA2	5'- GCA GTT AAA ATG GAA GGA CAC GAA CAC AC -3'	5'- GTA GTA GGA TGT GTC GGG TAT AGA TGC AGA -3'
nkx2.3	5'- ACA ATG ATT CCA AGT CCG ATT CTA GCT TCC -3'	5'- TTA CCA TGC CCT GAT CCC CTG CAG AGT TCC -3'
tbx1	5'- ATA CCT ACA ACT ATC CGG GAT CCA ATT CGG -3'	5'- ATT CAT GTG GTG ATG ATA CGT GTG TCC TCT -3'
tcf21	5'- AGT GAG GTT TCC ATG AGC GCA CAG GCG TAT -3'	5'- ATA AAA CAA ACA GGA ACC CGA ATG AAG TAC -3'
ripply2	5'- CAG ACT TTA CGA AGA GCT AAT CAG CGC AAG -3'	5'- CAA TGC TGC TAG TAG AAA TGA GTG CTC TGT -3'
wnt11r	5'- ATG AAG AGC CGC TCT CAC ATC CTG CCT GTT -3'	5'- GGT TGC TGG CAG GAG CAC AGG CCT ATT TGC -3'

Table S2. Defects of pharyngeal cartilages in *pax1* mutants (n=28)

Cartilage phenotype	CB1-4	CB5	CH	HS	PQ	BB
Absent	28	0	0	0	0	0
Shape change	-	9	4	27	2	28
Fusing to other cartilage	-	2 (to BB)	13 (to HS)	13 (to CH), 2 (to PQ)	2 (to HS)	2 (to CB)

BB, basibranchial; CB, ceratobranchial; CH, ceratohyal; HS, hyosymplectic; PQ, palatoquadrate.